ANL-7924
LMFBR Fuels and Materials
Engineering and Development
(UC-79b)

ARGONNE NATIONAL LABORATORY
9700 South Cass Avenue
Argonne, Illinois 60439

CHEMICAL ENGINEERING DIVISION

BURNUP, CROSS SECTIONS, AND DOSIMETRY SEMIANNUAL REPORT

January—June 1972

by

R. P. Larsen, N. D. Dudey,
C. E. Crouthamel, A. D. Tevebaugh,
M. Levenson, and R. C. Vogel

September 1972

Previous reports in this series:

ANL-7824 January-June 1971
ANL-7879 July-December 1971

DISCLAIMER

TABLE OF CONTENTS

LIST OF FIGURES

LIST OF TABLES

CHEMICAL ENGINEERING DIVISION
BURNUP, CROSS SECTIONS, AND DOSIMETRY SEMIANNUAL REPORT
January-June 1972

by

R. P. Larsen, N. D. Dudey, C. E. Crouthamel,
A. D. Tevebaugh, M. Levenson, and R. C. Vogel

ABSTRACT

Research and development efforts of the burnup, cross sections and dosimetry programs in the Chemical Engineering Division of Argonne National Laboratory are reported for the period January to June 1972. Work is reported in the following areas: (1) development of an X-ray spectrometric method for the determination of the rare-earth fission products and application of this method to the determinations of burnup in nuclear fuels; (2) determination of fast fission yields of burnup monitors and other fission products; (3) a search for a spontaneously fissioning isomer of ^{241}Pu; (4) measurements of the tritium and alpha particle yields in fast-neutron fission of ^{235}U and ^{239}Pu; (5) evaluations of available data on the differential cross sections for the $^{56}Fe(n,p)^{56}Mn$ and $^{32}S(n,p)^{32}P$ reactions; and (6) measurements of both fission rates by solid-state track recorders and reaction rates by foil activation, in the Coupled Fast Reactivity Measurement Facility.

SUMMARY

A method has been developed for the determination of the principal rare-earth fission products - lanthanum, cerium, praseodymium, neodymium, and samarium - in which the assay is made by X-ray spectrometry, using terbium as internal standard. The method will be used for the determination of burnup of fast-reactor oxide fuels and the determination of fast fission yields. The analysis of synthetic burnup samples prepared from inactive fission-product elements and uranium has shown that the accuracy of the method is ±1%. The results of burnup determinations, obtained by this method on two irradiated fast-reactor oxide fuels, have been compared with those obtained by mass-spectrometric isotopic-dilution determinations of ^{148}Nd and total neodymium. The agreement was within 1% (relative) in one case and within 4% in the other.

Encapsulated samples of ^{233}U, ^{235}U, ^{238}U, ^{239}Pu, ^{240}Pu, and ^{241}Pu that were irradiated in EBR-II for four years are being analyzed to determine the fast fission yields of burnup monitors and other fission products. The number of fissions will be determined by measuring the decrease, about 25%, in the heavy-atom content of the capsules; the number of fission-product atoms will be determined using such analytical techniques as X-ray, mass, and optical spectrometry. Conditions have been established for separating the rare earths from the capsule material, namely, high-purity nickel, and its impurities.

A search was made for a spontaneously fissioning isomer of ^{241}Pu (half-life, 10 to 100 days) using a sample of ^{240}Pu that had been irradiated in EBR-II. After separation of the plutonium from other sample constituents, the number of fissions occuring in the plutonium was measured with mica fission-track counters over a period of 150 days. During this time, a change of <1% was observed in the spontaneous fission rate (which was primarily from ^{240}Pu). An upper limit was calculated for the number of spontaneous fissions due to an isomer of ^{241}Pu and, from this, upper limits were calculated for the capture cross section of ^{240}Pu to form this isomer. The effects of the existence of such an isomer on (1) fast-reactor operation and (2) neutron shielding during shipment of irradiated fuels are also discussed.

Studies of low-mass atom production (tritons and alpha particles) in fast-neutron fission of LMFBR fuel materials are continuing. Tritium yields for ^{235}U have been measured by both radiochemical and particle-identification techniques, and alpha particle energy spectra and yields have been measured by the particle identification technique. Results for fast- and thermal-neutron tritium yields for ^{235}U are reported and compared with literature values. Preliminary studies of the tritium and alpha yields from ^{239}Pu are also presented. The angular distributions of alpha particles relative to the massive fragments have been measured in spontaneous fission of ^{252}Cf.

Evaluations of the microscopic cross sections for the $^{56}Fe(n,p)^{56}Mn$ and $^{32}S(n,p)^{32}P$ reactions are presented. The evaluations are part of a task force effort to formulate cross section data for neutron dosimetry purposes.

In the dosimetry program, measurements of fission rates from ^{235}U, ^{239}Pu, and ^{237}Np have been made with solid-state track recorders in the Coupled Fast Reactivity Measurement Facility (CFRMF) and the results are compared with data obtained by fission-chamber measurements. Measurements have also been made in CFRMF by the foil-activation technique to determine reaction rates of importance to dosimetry studies. Results from the EBR-II mapping study (Runs 50-51) have been used to evaluate the accuracy of the experimental data and of selected fission yields. Conclusions regarding the status of fission-yield data for dosimetry purposes are presented.

I. DETERMINATION OF BURNUP BY X-RAY SPECTROMETRIC MEASUREMENT OF RARE-EARTH FISSION PRODUCTS

(R. P. Larsen, R. D. Oldham, R. V. Schablaske*)

Development work has been completed on a method for determining burnup in fast-reactor oxide fuels by X-ray spectrometric assay of the five principal rare-earth fission products--lanthanum, cerium, praseodymium, neodymium, and samarium. The use of the rare-earth group as a burnup monitor, compared with an individual nuclide, e.g., ^{148}Nd, has a number of advantages: (1) the fission yield is virtually independent of fissile nuclide; (2) the fission yield is the sum of a number of independently measured fission yields and is, therefore, more accurately known than that of an individual nuclide; (3) the fission yield is independent of neutron energy because the rare-earth fission products constitute nearly 50% of the heavy portion of the mass-yield curve; and (4) neutron capture reactions will not significantly alter the relationship between total number of atoms of rare earth fission products and the number of fissions. The latter advantage results from the fact that neutron captures by more than 85% of the rare-earth nuclides produce a nuclide of the same element, e.g., $^{143}Nd(n,\gamma)^{144}Nd$, or another rare-earth element that is measured, e.g., $^{139}La(n,\gamma)^{140}La$. ($^{140}La$ is a short-lived nuclide that decays by beta emission to ^{140}Ce.) The only capture reactions that could decrease the measured ratio of rare-earth atoms to fissions are $^{146}Nd(n,\gamma)^{147}Nd$ and $^{152}Sm(n,\gamma)^{153}Sm$. Both ^{147}Nd and ^{153}Sm decay by beta emission to isotopes of rare earth elements that are not measured. The only reactions that could increase the ratio of rare-earth atoms to fissions are $^{138}Ba(n,\gamma)^{139}Ba$ and $^{147}Pm(n,\gamma)^{148}Pm$; subsequent beta decay products are ^{139}La and ^{148}Sm, which are measured.

The effect of neutron capture on the ratio of rare-earth atoms to fissions would be highest at high burnup. At 10% burnup, the neutron capture cross section of one of these nuclides would have to be in the order of 600 mb to alter the ratio by 1%. Fast neutron capture cross sections of this magnitude are considered to be very improbable. Moreover, the fission yields of ^{146}Nd, ^{152}Sm, ^{138}Ba, and ^{147}Pm are all small relative to the fission yields of the rare-earth group.

Various aspects of the development of this method have been discussed in previous annual reports (ANL-7425, p. 194, ANL-7575, p. 178, and ANL-7675, p. 120). Since then, various modifications (discussed below) have been made to improve the method. The procedure, as presently devised, involves the following steps: (1) a known amount of terbium (a rare earth whose fission yield is less than 0.05%) is added to the sample as an internal standard; (2) the rare earths are separated from uranium, plutonium, and several of the high-activity fission products by anion exchange in strong hydrochloric acid; (3) the rare earths are precipitated with ammonium hydroxide; and (4) the rare earths are electroplated onto aluminum from a dimethyl sulfoxide-dilute nitric acid medium. Measurements of the individual fission-product and terbium X-ray intensities (L series) are made in an X-ray spectrometer using a tungsten-target tube operated at 56 kV and 64 mA, a continuously flushed helium optical path, a lithium fluoride crystal, and a proportional counter. The X-ray intensities are corrected for interelemental interferences, and the rare earth-to-terbium intensity ratios are calculated. From these ratios, the ratios obtained from electroplated standards, and the amount of terbium added to the sample, the amount of each

*Analytical Group, Chemical Engineering Division.

fission-product rare earth in the sample is calculated. These amounts are summed and divided by the fractional fission yield to obtain the number of fissions.

A. Improvements in Procedures

It was reported previously (ANL-7675, p. 121) that low and erratic results were obtained for cerium and praseodymium when a solution which simulated a 1% burnup sample (a mixture of uranium, plutonium, and inactive fission-product elements) was carried through the entire procedure. It was speculated that at some point in the separation procedure some separation of cerium and praseodymium from terbium was occurring. To test this possibility a mixture of rare earths was neutron-irradiated and the activity ratios of ^{140}La(40 h), ^{143}Ce(33 h), ^{142}Pr(19 h), ^{147}Nd(11 d), and ^{160}Tb(72 d) were measured gamma spectrometrically. The irradiated mixture was then carried through the entire procedure, and the ratios were measured after electrodeposition of the rare earths. A comparison of the two sets of gamma-activity ratios showed that the value of each ratio, e.g., ^{143}Ce to ^{160}Tb, for the electrodeposited sample was within 1% of the value obtained prior to the separation procedure. It was therefore concluded that separation of cerium and praseodymium from the other rare earths was not occurring.

The source of the difficulty in the cerium and praseodymium measurements has been traced to a variability in the X-ray background radiation. It has been established that x-y orientation of the aluminum plate has a small effect on the intensity of scattered white radiation (bremmstrahlung) from the X-ray tube and a large effect on both the absolute intensities and the ratio of the intensities of scattered characteristic tungsten X-rays, L_α and L_β. The variability of the white radiation affects the background that is subtracted from the praseodymium X-ray intensity; the variability of the characteristic tungsten radiation affects the cerium measurement. The second-order tungsten L_α X-rays occur at the same 2θ angle as the first-order cerium L_α. The reason for these effects is undoubtedly a diffraction phenomenon coupled with a nonrandom orientation of the aluminum crystals in the plate.

The background variability problem has been overcome by measuring the intensity of scattered tungsten L_α X-rays from a plate at various x-y orientations prior to the use of the plate in the analysis, noting the orientation at which this intensity is a minimum, and marking the plate so that during the rare-earth assay the plate can be properly oriented. Establishing the optimum plate orientation is a simple procedure that can be accomplished in about 2 min.

An increase in the sensitivity of the method has also been realized by incorporating a rare-earth hydroxide precipitation into the procedure. The modification was originally made in connection with the determination of rare-earth fission yields (see Section II.B.1) in which a separation of the rare earths from a large amount of nickel was required. (The special samples for determining fission yields were irradiated in nickel capsules.) Because of the very high (85 to 95%) recoveries of rare earths obtained with this procedure the precipitation step was incorporated into the procedure for the preparation of standards prior to electroplating. The X-ray intnesities obtained were about 20% higher than those from directly electro-

plated standards. The modified procedure for determining burnup now includes precipitating the rare-earth hydroxides with ammonia, washing with very dilute ammonia, removing the wash solution, and dissolving the rare-earth hydroxides in dilute nitric acid.

The rare-earth hydroxide precipitation also provides a separation from the fission products cesium, strontium, and barium. This separation reduces the total amount of activity on the rare-earth plates and eliminates the correction that previously had to be made for the effects of cesium and barium on the measured X-ray intensities.

B. Analysis of Standards

Two synthetic samples, each of which contained 20 mg of uranium and amounts of inactive fission-product elements which simulated a 2% burnup sample, were analyzed for the rare earths using a procedure which incorporated the revisions discussed above. The results are given below:

Rare Earth	Amount Added, μg	Recovery, % Sample I	Sample II
La	19.5	97.3	97.5
Ce	41.0	100.8	101.8
Pr	19.7	102.7	101.6
Nd	54.7	99.0	98.9
Sm	8.5	94.8	97.3
Total	143.3	99.6	99.9

C. Comparison of X-ray and Mass-Spectrometric Methods--Analyses of High-Burnup UO_2-PuO_2

The X-ray method was proof-tested by determining the burnup of two samples of highly irradiated uranium-plutonium oxide; burnups were calculated both from total rare-earth content and from neodymium content. Table 1 compares these results with measurements of burnup based on the content of ^{148}Nd and total neodymium, both of which were determined by mass-spectrometric isotopic-dilution (MSID) analysis. (The MSID measurements of burnup were performed by J. E. Rein and R. M. Abernathy of Los Alamos Scientific Laboratory).

Although these samples were analyzed before the problem in background variation was recognized, this does not appear to be the explanation for the small discrepancies between the X-ray and MSID results on sample R-2680. The largest difference is in the neodymium burnup values, 8%. This is unexpected since these values should agree most closely. With the exception of mass 144,* both methods measure the same nuclides. In the development

*In the neodymium X-ray method the amount of ^{144}Ce (284 d) which has not decayed to ^{144}Nd is determined gamma spectrometrically and this number of atoms, about 10% of the measured neodymium, is added to the measured neodymium value.

TABLE 1. Comparison of Methods of Burnup Analysis

Sample No.	Burnup Monitor	Analytical Method	Burnup, %
R-2679	^{148}Nd	MSID	9.13
	Neodymium[a]	MSID	9.30
	Neodymium[b]	X-ray	9.11
	Total Rare Earths	X-ray	9.03
R-2680	^{148}Nd	MSID	7.40
	Neodymium[a]	MSID	7.25
	Neodymium[b]	X-ray	7.85
	Total Rare Earths	X-ray	7.70

[a]Masses 143, 145, 146, 148, and 150.
[b]Masses 143, 144, 145, 146, 148, and 150.

of the X-ray method, the difference between the known and measured neodymium values has never exceeded 3%. Since the burnup value determined for this sample by X-ray spectrometric assay of total rare earths is also somewhat higher than the two MSID values, it appears likely that the inconsistencies are related to some unresolved problem in handling the sample prior to analysis. An earlier comparison (see ANL-7675, p. 122) of the X-ray and MSID methods (MSID determination made by B. F. Rider of General Electric-Vallecitos) showed agreement comparable to that obtained on sample R-2679.

Additional comparisons of the two methods will be made during the fission-yield measurements program, particularly on samples from the long-term irradiation in EBR-II (See Section II).

II. FAST FISSION YIELDS OF BURNUP MONITORS
(R. P. Larsen, R. D. Oldham)

The determination of the fission yields of burnup monitors for FFTF and demonstration-reactor fuels has been initiated. The materials for these determinations are encapsulated samples of ^{233}U, ^{235}U, ^{238}U, ^{239}Pu, ^{240}Pu, and ^{241}Pu that were irradiated in EBR-II from December 1966 to September 1970. The subassembly containing the samples occupied a position in Row 2 for the first half of the irradiation and a position in Row 4 for the second half. Two sets of samples were irradiated: one in the core and the other in the axial blanket. The samples were irradiated at these two reactor positions to enable an evaluation to be made of the relationship between fission yield and neutron energy in fast reactors. The evaluation of this relationship using samples that were irradiated in the mockups of EBR-II, performed in ZPR-3 (Assemblies 60 and 61), showed that the difference in the fission yields is negligible in going from a neutron spectrum in the EBR-II core (Row 2) to a neutron spectrum in the radial blanket (Row 12) (see ANL-7775, p. 101 and ANL-7875, p. 16). Fission-yield determinations will, therefore, not be made on samples irradiated in the axial blanket. (The neutron spectrum in Row 12 of the radial blanket is comparable to that of the axial blanket in which the 4-yr irradiation was carried out).

The samples irradiated in EBR-II will be chemically analyzed to establish (1) the fast fission yields of burnup monitors for fast reactors as well as the yields of other fission-product nuclides that are of interest to the fast-reactor program, e.g., the krypton and xenon isotopes, and (2) the isotopic abundances of nuclides formed by nonfission nuclear transformations. The latter measurements will be made for nuclides whose fission yields are being determined as well as for ^{232}Th and ^{237}Np, which were also included in the long-term irradiations.

A. Determination of Number of Fissions

Table 2 summarizes the principal nuclear reactions that occurred during the EBR-II irradiation and the percentages of uranium and plutonium that underwent these reactions. It is seen that, with exception of ^{238}U, the percent fission of each nuclide is 10% or more. Because the relative decreases in the actinide atom contents are large and because the actinide atom contents (pre- and post-irradiation) of the capsules can be determined accurately (±0.1% or better), the number of fissions can be determined with an accuracy of ±1% or better. At the time of the encapsulation, the material loaded into each capsule (about 100 mg) and archive samples of each material were accurately weighed. When an irradiated capsule is dissolved for the fission-yield determinations, the archive samples will also be dissolved and these solutions will be analyzed for their actinide content. From the actinide atoms content of the archive samples and the weights of archive and encapsulated materials, the pre-irradiation actinide atom content of the irradiated capsule will be calculated. The difference between this value and the post-irradiation actinide atom content represents the number of fissions that occurred.

To determine the number of fissions that occurred in the ^{233}U, ^{235}U, ^{239}Pu, and ^{240}Pu capsules, the only measurements that must be made with a high degree of accuracy are the number of atoms of uranium (or plutonium)

TABLE 2. Nuclear Reactions in the EBR-II Irradiation (irradiation time = 45 months; fluence = 1 x 10^{23} neutrons)

Nuclide Irradiated	Reaction, at. %		
	Fission	(n,γ)[a]	Other
^{233}U	30	2 (^{234}U)	<0.1
^{235}U	22	4 (^{236}U)	<0.2
^{238}U	1.5	2 (^{239}Pu)	0.3 (^{239}Pu fission)
^{239}Pu	24	3 (^{240}Pu)	0.2 (^{240}Pu fission)
^{240}Pu	10	3 (^{241}Pu)	0.3 (^{241}Pu fission); 0.4 (^{241}Pu beta decay)
^{241}Pu	22	2 (^{242}Pu)	25 (^{241}Pu beta decay)

[a]The nuclides in parentheses are the capture products.

in the archive and irradiated samples and the isotopic compositions. Both of these measurements are obtained in the same analysis, which is performed by mass-spectrometric isotopic dilution. From the percentages given in Table 2, it is seen that for these four nuclides, >97% of the reactions that occurred in the irradiation were fissions and (n,γ) transformations. The products of the (n,γ) transformations, ^{234}U, ^{236}U, ^{240}Pu, and ^{241}Pu, respectively, all have half-lives of such lengths that radioactive decay to an isotope of some other element is either negligible (^{234}U, ^{236}U, and ^{240}Pu) or very small (^{241}Pu) relative to the sum of the fissions and (n,γ) transformations. The magnitudes of the other nuclear reactions that occurred, e.g., $^{236}U(n,\gamma)^{237}Np$ in the ^{235}U samples, are very small (less than 0.2 at. %). The corrections for all these reactions can be made by radiochemical determinations of the products.

To determine the number of ^{241}Pu fissions, accurate measurements of the ^{241}Am contents of the archive and irradiated samples will have to be made in addition to the plutonium measurements (^{241}Am is formed from beta decay of ^{241}Pu). The ^{241}Am measurements will also be made by mass-spectrometric isotopic-dilution analysis.

The number of fissions in the ^{238}U samples will be determined from their ^{137}Cs contents and the ^{238}U fast fission yield of ^{137}Cs. The fast fission yield of ^{137}Cs is presently being determined on samples of ^{238}U irradiated in EBR-II for 5 days at 60 MW. Separate samples from this irradiation are being analyzed for ^{140}Ba and ^{137}Cs. The number of fissions will be determined from the ^{140}Ba content and the previously determined fission yield of ^{140}Ba (see ANL-7879, p. 15); the fission yield of ^{137}Cs will be determined from the ^{137}Cs content and the number of fissions.

In the long-term irradiation of ^{238}U, about 20% of the total fissions were from ^{239}Pu, which is formed from the reaction $^{238}U(n,\gamma)^{239}U$ and subsequent decay to ^{239}Pu. The ^{238}U samples will be analyzed for ^{239}Pu, and appropriate corrections will be made for the fission products formed in ^{239}Pu fission. It is estimated that the accuracies of the ^{238}U fission yields obtained will be ±5%. Because the fraction of the total fissions due to ^{238}U in a fast reactor fuel (for example, at core center of FFTF), will be, at most, 0.07, this accuracy will meet the need for a burnup determination having an accuracy of ±1 to 2%.

B. Fission-Product Measurements

The fission yields to be determined are, in order of importance, (1) the yields of the nuclides that can be used as burnup monitors for oxide fuels, (2) the yields of nuclides that are important for other reasons in the operation of FFTF and demonstration reactors, and (3) the yields of burnup monitors for other fast-reactor fuels, e.g., carbides. The burnup monitors of interest for fast-reactor oxide fuels are the nuclides of the rare earths--lanthanum, cerium, praseodymium, neodymium, and samarium--and zirconium. The fission yields that are important to reactor operation are, for example, the xenon isotopes (mass $\leq$ 130) that are used as tags in detecting failed fuel elements. The burnup monitors of principal interest for carbide fuels are the nuclides of molybdenum and technetium.

Determination of the Rare-Earth Fission Products. The X-ray spectrometric method for fission-product rare earths (described in Section I) will be used to determine the rare-earth elemental contents of the samples irradiated in EBR-II; the isotopic distributions of the cerium, neodymium, and samarium will be established by mass spectrometric analysis of the rare earths separated for the X-ray spectrometric analysis (lanthanum and praseodymium are monoisotopic).

To execute the X-ray spectrometric determination, a procedure had to be devised for separating the rare earths from the capsule material, high purity nickel, and its minor impurities. The ratio of nickel to actinide content is about 70 to 1 (7 g of nickel and 100 mg of uranium or plutonium); the ratios of nickel to a high-yield (6%) fission product range from about 10,000 to 100,000. Thus, the procedure has to be capable of separating the rare earths from a large amount of nickel, in some cases as much as 1 g, without loss of rare earths, and from minor impurities in the nickel which interfere in the rare-earth determination. Impurities that follow the rare earths in the separation procedure and are electroplated, if present in the nickel at even the 10 ppm level, could affect the measurements. In the X-ray spectrometric method for the rare earths, the mass-absorption effect could be larger for one rare earth than another. The energies of the L X-rays of the rare earths are quite low (about 5 keV) and the lanthanum energy is about 40% lower than that of the internal standard, terbium.

Separation of the rare earths from nickel is satisfactorily accomplished by a preliminary precipitation of rare-earth hydroxides with ammonia. The actinides are also precipitated; the nickel, which forms a soluble complex with ammonia, remains in solution. Because some nickel is occluded in the precipitate, the precipitate is dissolved in hydrochloric acid and the actinides and rare earths are reprecipitated. When the modified procedure was tested with a synthetic solution containing 700 mg of nickel, 10 mg of uranium, and amounts of the inactive fission-product elements to make the solution equivalent to a 3% burnup sample, it was found that manganese and titanium impurities in the nickel were not separated. The amounts of these elements electroplated with the rare earths resulted in significant mass absorption of the rare-earth X-rays. This problem was overcome by modifications in the ion-exchange step, in which the actinides and some fission products are separated from the rare earths. The hydrochloric acid concen-

tration was increased from 12 to 14M and the length of the ion-exchange column was doubled. Titanium and manganese were adsorbed with the uranium and thus separated from the rare earths. These additional separation steps resulted in a substantial decrease in the amounts of rare earths electroplated. (Although quantitative recovery is not necessary when an internal standard is used, very low recoveries affect the accuracy of the X-ray measurements). Other techniques for mounting the rare earths, e.g., pipetting onto Millipore filters and drying, were investigated, but the results obtained were erratic.

A precipitation of the rare-earth hydroxides after the ion exchange step resulted in high recoveries in the electrodeposition step. Small amounts of impurities, such as ammonium ions which could form as the result of degradation of the ion-exchange resin, are known to impede the electrodeposition process. The precipitation of the rare-earth hydroxides effects a separation from these contaminants and again enables a high percentage of the rare earths to be electroplated. The hydrochloric acid solution of the rare earths from the ion-exchange column is evaporated to dryness, the rare earths are dissolved in dilute nitric acid, and strong NH_4OH is added to precipitate the rare-earth hydroxides. After centrifugation, the supernate solution is drawn off, the rare-earth hydroxides are washed with very dilute NH_4OH and centrifuged, the supernate is drawn off, and the hydroxides are dissolved in very dilute nitric acid. Dimethyl sulfoxide is added and the rare-earths electroplated.

In summary, the procedure devised for measuring the rare-earth contents of the fission-yield samples involves (1) separation of the rare earths and actinides from nickel by precipitation with NH_4OH, (2) ion-exchange separation of rare earths from uranium and plutonium and impurities in the nickel (maganese and titanium), (3) precipitation of rare-earth hydroxides with NH_4OH, and (4) electroplating of rare earths from a dimethyl sulfoxide-dilute nitric acid solution. The overall recoveries of the rare earths in this procedure are 80 to 90%.

III. SEARCH FOR A SPONTANEOUSLY FISSIONING ISOMER OF ^{241}Pu
(R. P. Larsen, R. D. Oldham)

A sample of ^{240}Pu from our 4-yr irradiation in EBR-II has been used to conduct a search for a short-lived, spontaneously fissioning ^{241}Pu isomer, $^{241m}Pu_{SF}$. The possibility of the existence of such an isomer, which would be formed by the reaction $^{240}Pu + n \rightarrow {}^{241m}Pu_{SF}$, has been receiving considerable attention recently.

In a study to determine the half-life of ^{241}Pu, Nisle and Stepan[1] made reactivity measurements over a 3-yr period on a sample of ^{241}Pu of high isotopic purity. The results of their measurements showed that there were two components of the ^{241}Pu decay curve (log of reactivity versus time): a component having a half-life of 0.34 ± 0.11 yr and a component having a half-life of 14.63 ± 0.27 yr. Previously reported values for the half-life of ^{241}Pu varied from 13 to 15 yr. Two explanations have been put forth to account for the results: (1) the existence of a short-lived isomer of ^{241}Pu, namely, ^{241m}Pu, which decays either by beta emission to ^{241}Am or by gamma emission (internal transition) to ^{241}Pu (14.63 yr) and which has an extremely high fission cross section relative to that of ^{241}Pu; and (2) the existence of a short-lived isomer of ^{241}Pu, namely, $^{241m}Pu_{SF}$, which decays by spontaneous fission. The latter explanation, suggested by Nilsson and co-workers,[2] prompted the present study.

If $^{241m}Pu_{SF}$ exists and has a half-life greater than a few seconds, it would be important not only to fission-process theorists, but could also have considerable practical consequences. If the half-life is in the range of minutes to hours and the cross section for the reaction $^{241}Pu + n \rightarrow {}^{241m}Pu_{SF}$ is sufficiently large, reactor control during shutdown could be affected. At the present time, shutdown is, in part, governed by delayed-neutron emission by short-lived fission products. (These neutrons induce fission and therefore, the generation of heat continues.) If the neutron emission rate from a spontaneously fissioning isomer of ^{241}Pu were equal to or greater than 10% of the delayed-neutron emission rate, reactor shutdown procedures in a plutonium-fueled fast reactor would be affected.

Another governing factor in reactor shutdown is fission-product decay heat. This constitutes about 6% of the total heat just before the end of a prolonged power run and about 0.6% an hour after shutdown. If the heat produced by the fission of $^{241m}Pu_{SF}$ were significant, relative to the fission product heat, this might also constitute a factor important to reactor shutdown.

A long-lived spontaneously fissioning isomer of ^{241}Pu could have an important effect of the design of fuel shipping casks. If the half-life is of the order of 10 days or more and the cross section for the formation of the $^{241m}Pu_{SF}$ is high enough, the neutron-emission rate of irradiated fast-reactor fuel during shipment from the reactor to the processing plant could be significantly higher than the rate calculated from the spontaneous fission of ^{242}Cm and ^{244}Cm. The design of shipping casks to meet federal regulations with respect to neutron emission rates is presently based on the expected concentrations of these curium isotopes in the irradiated fuel.

A. Experimental Work

As stated previously, our search for $^{241m}Pu_{SF}$ was made using a ^{240}Pu sample that had been irradiated in EBR-II for four years. The sample was discharged from the reactor in September 1970. This sample was considered a good choice for this search because it had been subjected to a fast flux of high intensity [2×10^{15} n/(cm^2)(sec)] over an extended period prior to a discharge from the reactor. (It has been postulated that if the spontaneously fissioning isomer is formed, the probability of formation in a fast flux is much higher than in a thermal flux.) The only disadvantage with the sample was that ∿200 days had elapsed between reactor discharge and the initial assay for fission events.

In preparation for assay by fission-track counting, the irradiated ^{240}Pu sample, along with its nickel capsule, was first dissolved, and a portion of the solution was converted to a nitric acid medium. The plutonium was then oxidized to the hexavalent state with argentic oxide, aluminum nitrate salting solution was added, and the plutonium was extracted into hexone. This procedure separated the plutonium from nickel and from transplutonium isotopes, some of which decay by spontaneous fission. A portion of the hexone solution was stippled onto a platinum plate in a manner to produce a reasonably uniform spread over an area of about 3 cm^2. The hexone was evaporated and the plate heated to about 700°C.

This plutonium (7.35 μg of ^{240}Pu) was contacted by a succession of mica fission-track recorders for progressively longer periods of time from April 1971 to October 1971. The number of fission tracks per day in the first period (14 days) was 198 ± 7 (2σ) and in the last period (31 days) was 203 ± 4 (2σ). Within the statistical limitations of the data (calculated on the basis of the total number of fission events recorded) there was no change in the number of fissions per day over the 150-day period in which measurements were made.

B. Discussion and Conclusions

It is concluded that all the fission events recorded were due to the spontaneous fission of $^{240}Pu[t_{1/2}(SF) = 1.34 \times 10^{11}$ years]. The calculated number of fission tracks from 7.35 μg of ^{240}Pu is 245 per day. The difference between this value and the average measured value, 201, may be due to an error in the half-life or may be due to the solids on the plate. The deposition of plutonium was not completely uniform and some other solids could have been present. (The presence of solids has the effect of reducing the optical efficiency of a track recorder.) From the fission-track measurements it has been conservatively estimated that the number of spontaneous fissions due to $^{241m}Pu_{SF}$ would have to be less than 1.3 per day per microgram of the irradiated ^{240}Pu.

The upper limits of the cross section of the reaction $^{240}Pu + n \rightarrow {}^{241m}Pu_{SF}$ have been caluclated for half-lives of $^{241m}Pu_{SF}$ ranging from 6 to 200 days. These calculations were based on the following: an upper limit of 1.3 fissions per day per microgram of ^{240}Pu for the spontaneous fission rate of $^{241m}Pu_{SF}$, an irradiation time of 30 days (the last power run before discharge of the sample from EBR-II), a flux of 2×10^{15} n/(cm^2)(sec), and an out-pile time of 200 days. The results are given in the following table:

$^{241m}Pu_{SF}$ Half-Life, d	Cross Section, b
6	$<5 \times 10^{-2}$
12	$<4 \times 10^{-7}$
25	$<2 \times 10^{-9}$
50	$<3 \times 10^{-10}$
100	$<2 \times 10^{-10}$
200	$<3 \times 10^{-10}$

As mentioned above, the formation of a short-lived, spontaneously fissioning isomer of ^{241}Pu could, if the cross section were high enough, result in a neutron shielding problem during shipment of fast reactor fuel from the reactor to a fuel processing plant. On the basis of available data[3] an LMFBR fuel that has been irradiated to 8% burnup and cooled for 100 days will have a curium spontaneous-fission rate of 3×10^5 fissions/(sec)/(g of plutonium). From the ^{240}Pu concentration in this fuel, a neutron flux of 10^{16} n/(cm^2)(sec), and the upper limits of the ^{240}Pu cross sections in the above table, upper limits were calculated for $^{241m}Pu_{SF}$ fissions/(sec)(g of plutonium). These values are given in the follwing table for the various assumed half-lives of this isomer:

$^{241}Pu_{SF}$ Half-Life, d	$^{241}Pu_{SF}$ Fissions/(sec)(g Pu)
6	$<3 \times 10^{11}$
12	$<3 \times 10^{6}$
25	$<1 \times 10^{4}$
50	$<1 \times 10^{2}$
100	$<3 \times 10^{2}$
200	$<3 \times 10^{2}$

If the $^{241m}Pu_{SF}$ has a half-life greater than 25 days, the ^{240}Pu cross section (see above) is such that the amount of $^{241m}Pu_{SF}$ relative to ^{242}Cm and ^{244}Cm in a fast reactor fuel is negligible. If the $^{241m}Pu_{SF}$ has a half-life of less than 25 days, its effect on fuel shipment or reactor shutdown cannot be assessed on the basis of the available data.

IV. FAST-NEUTRON FISSION YIELDS OF TRITIUM
(N. D. Dudey, M. J. Fluss, R. L. Malewicki)

The purpose of this program is to establish the information necessary for predicting tritium production rates in LMFBRs and for estimating the tritium burden of reactor and fuel-reprocessing plants. Of particular importance is the measurement of the fission yield of tritium as a function of neutron spectrum and fissioning nuclide. Two independent methods have been implemented for establishing tritium yields. The first method is a radiochemical technique in which the tritium is separated from an irradiated target and counted. The second uses a direct, on-beam particle-identification technique for measuring the number and energy of all low-mass particles (^{1}H, ^{2}H, ^{3}H, ^{3}He, ^{4}He, and ^{6}He) emitted from a fissile target. Both techniques involve irradiation of the fissile nuclides in a beam of monoenergetic neutrons at several neutron energies. During this reporting period, work on both methods has emphasized the measurements of tritium yields from fast-neutron fission of ^{235}U as a function of neutron energy; feasibility studies for measuring low-mass yields from ^{239}Pu fission were also made by the particle-identification technique.

A. Radiochemical Method

The radiochemical method involves (1) hydriding an irradiated sample to provide exchange between tritium and natural hydrogen, (2) dehydriding the sample, (3) separating the hydrogen by pumping it through a silver-palladium valve, which is permeable only to hydrogen isotopes, and (4) counting the tritium in a low-level gas proportional counter. The radiochemical measurements to date have been limited in accuracy by the number of tritium atoms produced in a given irradiated sample. However, the higher beam currents recently available on the Dynamitron (500 μA instead of 200 μA), combined with an improved lithium-target cooling system, have enabled us to increase the tritium level in irradiated samples by a factor of three. Furthermore, we have also been able to make measurements at much lower neutron energies.

During this reporting period, samples of ^{235}U, ^{239}Pu, and ^{233}U were irradiated at neutron energies of 140, 390, 590, and 800 keV, and samples of ^{235}U and ^{239}Pu were irradiated at a nominal neutron energy of 50 keV. Uranium-235 fission chambers were used to monitor the flux and fluence levels, and gold wires were used to map the neutron flux distribution for each of the irradiations. The absolute number of fissions that occurred in each sample was determined by Ge(Li) counting of the fission products ^{140}Ba, ^{103}Ru, and ^{95}Zr.

Tritium separation and counting of five previously irradiated samples (ANL-7879, p. 23) have been completed. These samples were irradiated at neutron energies between 250 and 450 keV in the Fast Neutron Generator of the Applied Physics Division. Even though these irradiations were for six days, the low flux intensity that was available allowed tritium yields to be determined only at 380 keV; the value measured was $1.90 \pm 0.17 \times 10^{-4}$ tritons/fission (T/f). Tritium separation of five ^{239}Pu samples was also completed and the samples are currently being counted.

B. On-Beam Particle-Identification Method
(M. J. Fluss, N. D. Dudey)

This method differs from the radiochemical technique in that all low-mass charged particles emitted during fission are detected and identified on-line and the kinetic energy of each particle is determined. The data obtained in this program will aid in understanding the mechanism of low-mass particle production in fission; however, our major interest is in understanding the dependence of tritium production in fast-neutron fission on neutron energy and fissioning species. Accordingly, two types of fission are being studied: spontaneous fission (e.g., of ^{252}Cf) and monoenergetic-neutron-induced fission of ^{235}U and ^{239}Pu over the energy range 200-4000 keV. Initially, efforts have been focused on measuring the number of particles emitted per fission and the energy distributions of ^{1}H, ^{2}H, ^{3}H, ^{3}He, ^{4}He, and ^{6}He as a function of neutron energy for ^{235}U.

The technique of particle identification (see ANL-7879, p. 23) takes advantage of the differences in the rate of energy loss of charged particles as a function of their charge and mass. By the use of a two-detector telescope having a thin (ΔE) and a thick (E) detector, a particle traversing the telescope will generate signals in the detectors that are proportional to the energy lost in each detector. The two energy signals resulting from this traversal are such that the total kinetic energy of the particle is ($\Delta E + E$); the relationship between ΔE and ($\Delta E + E$) uniquely defines the mass and charge of the particle.

In a series of experiments on the Physics Division's Dynamitron, our measurements of ^{235}U were completed and preliminary measurements of ^{239}Pu were begun. Measurements of tritium and alpha-particle yields for ^{235}U were made at six neutron energies between 200 and 500 keV. Within the uncertainty of each measurement (±10-15%), the tritium yields measured in this series of experiments were identical to previous particle-identification and radiochemical results. Alpha-particle spectra and yields were measured simultaneously with triton spectra and yields. The alpha yields were reasonably constant and were similar to available thermal-neutron yield values of $\sim 2 \times 10^{-3}$ alpha particles per fission. The alpha-particle energy spectra were typical of long-range alpha spectra except at energies of about 400 keV. This is the third independent series of experiments in which we have observed anomalous energy spectra (spectra composed of two distinct peaks or components as opposed to the normal single peak) in this neutron-energy region.

Our preliminary studies of ^{239}Pu were very encouraging. A uniform (2 mg/cm^2) target of ^{239}Pu was prepared by electrodeposition. Measurements of tritium and alpha-particle spectra were made at four neutron energies. Although the data have not as yet been fully analyzed, preliminary indications are that (1) both energy spectra peak about 1 to 2 MeV higher than the corresponding spectra for ^{235}U and (2) alpha and tritium yields are similar to the reported thermal-neutron yield values for ^{239}Pu. This is in contrast to our tritium data for ^{235}U, in which the fast-neutron yield is about 2.5 times the thermal yield (see Section C below).

C. ^{235}U Tritium Yields

The results of all measurements of fast-neutron tritium yields for ^{235}U, obtained by both methods, are presented in Fig. 1. The uncertainty of each individual measurement was assigned by a propagation-of-error analysis. For the radiochemical measurements, the uncertainties included tritium counting statistics (for both the sample and background), determination of the number of fissions, and tritium counting efficiency;

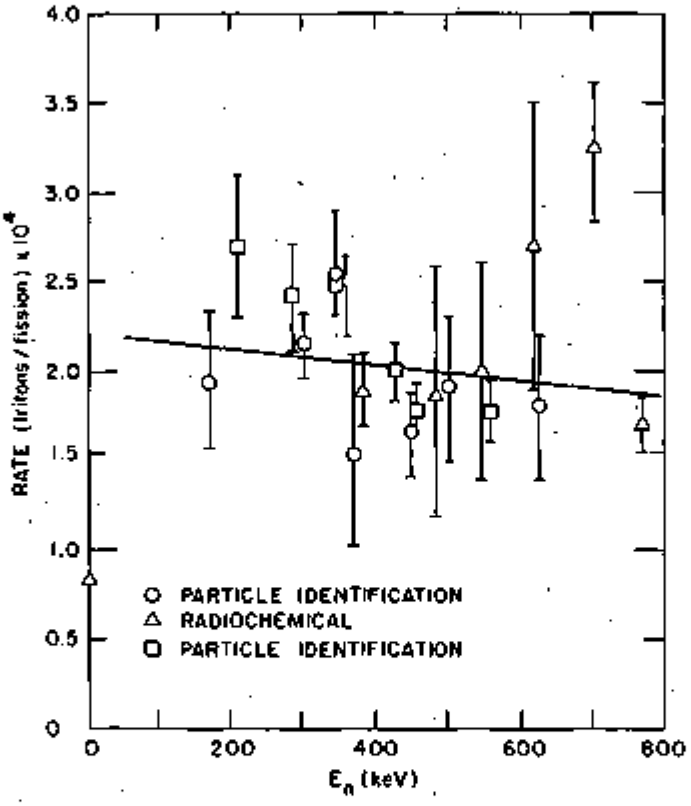

Fig. 1. Tritium Yields from Fast-Neutron Fission of ^{235}U.

for the particle-identification experiments, the principal uncertainties were particle-detection efficiency, fission-fragment counting efficiency, resolution of tritons from other fragments, and counting statistics. The solid line in Fig. 1 is a linear least-squares fit of all the data, weighted by the uncertainty of each individual measurement.

Better fits to the data were obtained with higher order polynomial functions; however, the relatively large uncertainties in each datum point made such procedures misleading. Any energy dependence in the tritium yields over this energy range is obscured by the uncertainty of the data. The linear fit indicates a slight tendency for the yield to decrease with increasing energy. With only one exception, all measurements are within 2σ of the fitted line. The agreement between the two techniques is quite satisfactory, e.g., a weighted fit of only the radiochemical data is within 5% of either of the two series of particle-identification experiments.

A summary of available literature data[4-7] on tritium yields from thermal-neutron fission of ^{235}U, as well as our experimental data on thermal yields, is given in Table 3. The average value of the results, which were obtained by three very different techniques, is 0.90×10^{-4} tritons per fission with a standard deviation of ±6% about the mean. Thus, the tritium yields presented in Fig. 1 for the neutron energy region from 200 to 800 keV are higher than the thermal neutron yield by a factor of two to three. This increase is contrary to theoretical predictions,[8,9] and raises some interesting implications regarding tritium production in the current generation of thermal reactors. Estimates of tritium production rates in light-water thermal reactor fuels are based upon tritium yields ranging from 0.8 to 1.2×10^{-4} T/f. Even in thermal reactors, a significant fraction of the fissions occurs from epithermal and higher-energy neutrons. If the tritium yield is also high in the epithermal region, the use of these yield values may result in underestimation of tritium production in thermal reactors. Extrapolation of our data to lower neutron energies suggests that this is indeed a possibility, yet we know that, at some energy, the yield must decrease to the thermal value. Measurements appear to be needed to define tritium yields in the neutron energy range between thermal and 200 keV.

TABLE 3. Tritium Yields for Thermal Fission of ^{235}U

Tritium Yield, 10^{-4} T/f	Method		Ref.
	Separation	Counting	
0.5-1	Radiochemical	Liquid scintillation	4
0.95±0.08	Radiochemical	Liquid scintillation	5
0.80±0.10	Radiochemical	Liquid scintillation	6
1	Particle identification	Particle counting	7
0.85±0.09	Physical	Internal gas proportional counting	This work

It is of interest to examine the effects of these tritium-yield results upon tritium production in fast breeder reactors. Sehgal and Rempert[10] have calculated an annual tritium production rate in EBR-II of 187 Ci, assuming a tritium yield of 0.8×10^{-4} T/f, a reactor power level of 62.5 MW(t) and a load factor of 0.7. Our results indicate a spectrum-averaged fast-neutron tritium yield from ^{235}U of $2.1 \pm 0.2 \times 10^{-4}$ T/f for EBR-II. This represents a tritium production rate in EBR-II of 490 Ci/yr, or 2.6 times that estimated by Sehgal and Rempert.

D. Angular Distribution of Alpha Particles in ^{252}Cf Fission

As part of our efforts to understand the mechanisms of low-mass atom production in fission, we have collaborated with S. Kaufman and E. P. Steinberg of the Chemistry Division in measuring the angular distribution of alpha particles in ternary fission of ^{252}Cf. This work has been completed and a paper describing the work has been submitted for publication. The highlights of this study are presented below.

Once in every few hundred fissions, three charged particles are produced, in contrast to the more common two-fragment mode of fission. Energy and angular distributions associated with the special three-fragment (ternary) fissions show that the "third particle" (which is most commonly an alpha particle) is formed at some point between the two larger fragments within $\sim 10^{-21}$ sec of the time of scission. Information concerning the positions and momenta of the fission fragments at the time of scission can be derived from the width of the angular distribution of the alpha particles with respect to the direction of the fission fragments.

Two previously reported experiments[11,12] have yielded widely discrepant widths for the alpha-particle angular distributions for spontaneous fission of ^{252}Cf. We have studied this system by using a position-sensitive triode to measure the energy and angular distribution of the alpha particles simultaneously with the mass of one of the massive fission fragments. Improved angular resolution, combined with time-of-flight measurements of the massive fragment, has resulted in angular distribution data that are a significant improvement over previous measurements. Figure 2 shows our data for the angular distribution of alpha particles relative to the lighter of the two fission fragments and also gives a comparison of our data with the results from the two earlier experiments.[11,12] The quantity $N(\theta_L)$ is the relative number of alpha particles as a function of angle, the angle being measured relative to the light fragment.

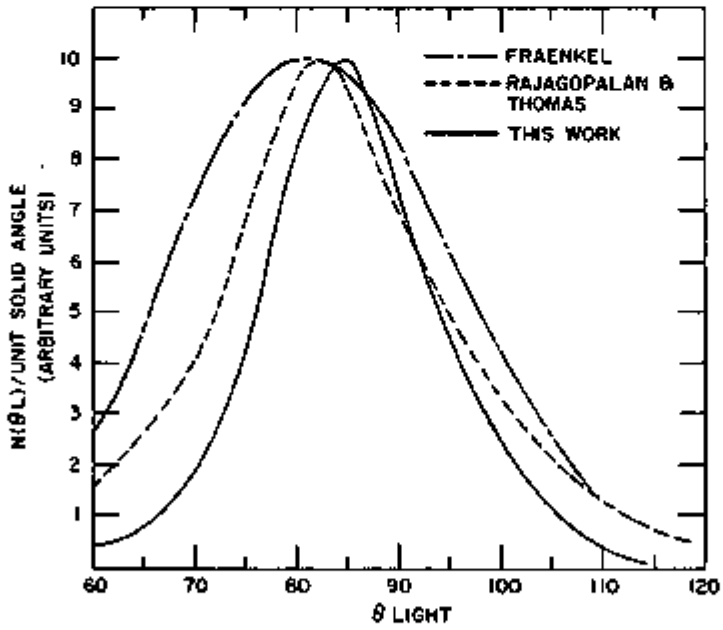

Fig. 2. Angular Distribution of Long-Range Alpha Particles Relative to Light Fission Fragments in the Spontaneous Fission of ^{252}Cf.

The width of the angular distribution is directly related to the total kinetic energy of the fragments at scission. Our measured value of 18.5° (full width at half maximum) corresponds to a total kinetic energy of the fragments of less than 7 MeV at the time of scission. This result is in disagreement with energy values of 40 MeV at scission that are predicted by the liquid-drop theory of fission.[13] Further studies of three-fragment fission should serve as an important guide to theorists in attempting to understand the dymanic processes of scission.

V. CROSS-SECTION EVALUATIONS

(N. D. Dudey, R. Kennerley*)

The Normalization and Standards Subcommittee of the Cross Sections Evaluating Working Group (CSEWG) of the AEC's Division of Reactor Development and Technology has been asked to review the status of multigroup activation cross-section sets which are used in the analysis of neutron dosimetry. To carry out this function the Subcommittee formed a task force to deal with microscopic cross-section data for neutron dosimetry purposes. Because of our participation in dosimetry activities, including the Interlaboratory LMFBR Reaction Rate Program (see Section VI), we were asked to represent Argonne National Laboratory (ANL) on this task force. Our initial responsibilities were to evaluate the available data on two reactions: $^{115}In(n,n')^{115m}In$ and $^{56}Fe(n,p)^{56}Mn$. Preliminary evaluations were prepared and presented at a task force meeting on March 29, 1972 at Battelle Northwest Laboratory. At this meeting it was decided that we should prepare a formal evaluation of the $^{56}Fe(n,p)^{56}Mn$ and the $^{32}S(n,p)^{32}P$ reactions, prepare the data in ENDF/B** format, and initiate, through the normal CSEWG framework, acceptance and testing of these evaluations. The ultimate objective is to incorporate the dosimetry cross sections into the ENDF/B data files. The evaluations that we prepared and submitted are presented in Appendix A.

*Participant in the Undergraduate Honors Research Program.

**ENDF/B is a file of evaluated nuclear data to be used for reactor design purposes. The file is maintained by Brookhaven National Laboratory.

VI. DOSIMETRY
(N. D. Dudey)

The objective of the dosimetry program is to develop experimental and analytical techniques for characterizing fast-neutron environments by means of activation rate measurements. A major part of our effort in this program is devoted to participation in the Interlaboratory LMFBR Reaction Rate (ILRR) Program. The specific aims of the ILRR Program are to (1) investigate systematic errors in foil-activation techniques, (2) reduce uncertainties in integral reaction-rate measurements, (3) intercompare techniques for neutron-spectral characterization, and (4) develop the capability for performing fission-rate measurements with an accuracy of ±3% (at the 95% confidence level). In addition to the work in the ILRR Program, we have the responsibility for establishing a capability for routine, coordinated dosimetry service for all ANL experimenters.

A. Interlaboratory LMFBR Reaction Rate Program: Dosimetry Methods Development
(N. D. Dudey, R. J. Popek)

ANL's responsibilities in the ILRR Program are to measure (1) absolute fission rates of ^{235}U, ^{238}U, ^{237}Np, and ^{239}Pu by means of solid-state track recorders (SSTR), (2) production rates of fission products for the same fissile materials, and (3) reaction rates for dosimetry foils; the latter two types of measurements are made by absolute gamma-ray counting. Measurements will be conducted in several well-established, permanent neutron fields; the first neutron field to be utilized is the Coupled Fast Reactivity Measurement Facility (CFRMF) at Aerojet Nuclear Corporation. Other laboratories will perform radiochemical measurements, fission-rate measurements, and neutronic calculations. The other laboratories participating in this program are Hanford Engineering Development Laboratory, National Bureau of Standards, Aerojet Nuclear Corporation, and Los Alamos Scientific Laboratory. Each participating laboratory reports progress in this program by quarterly contributions to an informal report "LMFBR Reaction Rate and Dosimetry Quarterly Progress Report." The highlights of the ANL contributions are summarized below.

1. Fission-Rate Measurements in CFRMF by SSTR

The SSTR technique involves placing a thin, uniform deposit of a fissile material in intimate contact with a suitable dielectric such as mica or synthetic materials such as Lexan or Macrofol. As fissions occur in the fissile material, the recoil fission fragments produce radiation damage tracks in the dielectric which, upon suitable chemical etching, are enlarged and are visible under a microscope. The principal errors in the technique are in (1) the determination of the number of fissile atoms, typically about 1.0%, and (2) the accuracy in counting tracks, typically 0.5%. Thus, the dominant uncertainty is in determining the number of fissile atoms exposed to the track recorder.

We are presently developing techniques for uniformly plating nanogram amounts of each of the four fissile materials (^{235}U, ^{238}U, ^{237}Np, and ^{239}Pu) onto platinum backing materials in such a way that the number of atoms plated can be established with maximum accuracy. First, stock solutions of known concentrations are prepared for each of the materials.

For this work, all new glassware is used. Also, since all chemical reagents are potentially contaminated with trace amounts of uranium, they are purified. Hydrochloric acid is purified by passing it through an anion-exchange resin, and nitric acid is prepared by redistillation. To date, solutions of ^{235}U, ^{239}Pu, and ^{237}Np have been prepared. For the ^{235}U solution, approximately 1 g of metal was first etched in acid to remove oxide, dried, and quickly weighed. (This large amount was required to assure that surface oxidation after cleaning would contribute a negligible error in the weight of metal.) The uranium was then dissolved in nitric acid and diluted to a convenient volume in a tared weighing bottle. The ^{239}Pu and ^{237}Np solutions were prepared similarly except that smaller amounts of material were dissolved. The isotopic compositions of the ^{235}U, ^{239}Pu, and ^{237}Np are given in Table 4.

TABLE 4. Isotopic Composition of SSTR Stock Solutions

^{235}U		^{239}Pu		^{237}Np		^{234}U	
^{235}U	93.12%	^{239}Pu	99.99%	^{237}Np	99.99%	^{234}U	99.885%
^{234}U	0.96%	^{240}Pu	8 ppm			^{235}U	0.064%
^{236}U	0.32%					^{236}U	0.035%
^{238}U	5.59%					^{238}U	0.014%
						^{232}U	<0.01%

The SSTR plates are prepared by electrodeposition of the materials onto platinum plates. The atom content of each plate must be determined as accurately as possible. Because the electrodeposition procedure may not be quantitative (within 0.5%), our technique is to alpha count each plate and relate that count to an alpha count of a known amount of stock solution. The atom content of the stock solution is well known and portions can be prepared for alpha counting by direct plating using a weight burette for the transfers. The accuracy of this method is limited primarily by the accuracy of the alpha counting, namely, counting statistics.

To reduce the counting uncertainty, it is necessary to spike the ^{235}U (and ^{238}U) with a small amount of an isotope with a high specific alpha activity. Uranium-234 was chosen as the spike material. The isotopic composition of the ^{234}U used is also given in Table 4. The stock solution of ^{234}U was prepared from a few milligrams of material by the method described above for ^{235}U. Since the ^{234}U contained trace amounts of ^{232}U (together with its alpha decay products), a purification was necessary to remove the alpha decay products. Separation from all the decay products except lead was accomplished by anion exchange. Lead-212 is not an alpha emitter but it has an alpha-emitting daughter. The ^{212}Pb (10.6 h) was allowed to decay and the ion-exchange procedure was repeated. Although this procedure does not remove ^{232}U, the rate of buildup of its daughters is known. During the first 25 days after the separation, the daughter products contribute less than 1% alpha activity relative to the ^{232}U. Since the amount of material on a plate is determined by relating its activity to that of the stock solution, the ^{234}U stock solution must be recounted every 2 to 3 weeks to establish an accurate value for the alpha activity.

The alpha activity of the stock solutions was determined by preparing four alpha plates of each solution by means of weight burette transfers and counting them with a 2Π gas-flow proportional counter. For the ^{235}U solution, this procedure provided the number of alpha counts per milliliter of solution and, thus, a direct measure of the number of atoms of ^{235}U on the plate. The agreement in four determinations was better than 0.5%; the accuracy of determining the number of atoms on the electrodeposited plates is estimated to be better than ±1%. The determination of alpha activity in the ^{239}Pu and ^{237}Np stock solutions was identical to that for the ^{235}U solution except that no alpha-activity spike was necessary. The accuracy of determining the number of atoms of plutonium and neptunium on the plates, which is limited by counting statistics, alpha contaminants in the solutions, and the accuracy of the half-life for alpha decay, is estimated to be ±0.8%.

Stock solutions of ^{235}U, ^{237}Np, and ^{239}Pu have been prepared as described. The ILRR program has now reserved large quantities of these materials as well as ^{238}U, all having very high isotopic purity. Prior to receipt of the high-purity ^{235}U material, no ^{238}U stock solutions were prepared. We now have high-purity ^{235}U and ^{238}U, and new stock solutions are now being prepared. In addition, we have obtained a quantity of ^{234}U that has been isotopically separated to remove ^{232}U as well as its alpha decay products. A stock solution of this material is also being prepared; hence, in future experiments no elaborate radiochemical processing of the ^{234}U will be required.

Track-recorder measurements in CFRMF for ^{235}U, ^{237}Np, and ^{239}Pu (using plates prepared by the procedure described above) were made on February 3 and 4, 1972. Fission-track counting has been completed for the ^{235}U and ^{237}Np packages; the ^{239}Pu samples are currently being counted. In the ^{235}U samples, corrections had to be made for fission tracks resulting from ^{234}U (3.16 at. %) and ^{238}U (5.59 at. %); these corrections were made assuming fission-rate ratios of $^{234}U/^{235}U = 0.417$ and $^{238}U/^{235}U = 0.047$.* The results for the ^{235}U and ^{237}Np fission-rate measurements are tabulated in Table 5.

This first track-recorder study in CFRMF had several objectives; these will be discussed individually. Firstly, we wanted to ascertain the degree of precision that could be obtained. For this purpose consider the following: Samples 5-10 and 5-11 were irradiated together, samples 5-12 and 7-7 were irradiated together, and samples 7-5 and 7-6 were irradiated together. The ^{235}U samples (5-10 and 5-11) agreed within 0.82%. The statistical fluctuation (uncertainty due to track counting) is expected to be about 0.9% (1σ). Thus the observed precision is comparable to the precision expected from counting statistics alone. Next we compare two ^{235}U samples (5-11 and 5-12) that were irradiated separately and two ^{237}Np samples (7-6 and 7-7) that were also irradiated separately. The ^{235}U samples agreed within 0.67% and the ^{237}Np samples within 0.62%. The standard deviation from the average of all three ^{235}U samples is 0.38% and that of the three ^{237}Np samples is 0.41%. Our conclusion is that the relative amounts of material on each track recorder are established to considerably better than ±1%.

*The $^{238}U/^{235}U$ fission-rate ratio was measured by J. Grundl of the National Bureau of Standards (NBS) in the CFRMF reactor as part of the ILRR program; his measurements were made by means of back-to-back fission chambers. No corrections were required for the ^{237}Np track recorder results.

TABLE 5. Fission-Rate Data Measured by SSTR at the Center of CFRMF

Sample Number	Irradiation Number	Isotope	Weight, ng	Exposure Time, sec	Fission Rate, 10^{-15} fissions/(atom)(sec)
5-10	4	^{235}U	99.7	3605	13.07
5-11	4	^{235}U	98.2	3605	13.21
5-12	7	^{235}U	86.2	3609	13.23
					13.17±0.05
7-1	8	^{237}Np	3410	368	4.94
7-2	9	^{237}Np	3509	371	4.83
7-5	6	^{237}Np	352	2948	4.84
7-6	6	^{237}Np	324	2948	4.88
7-7	7	^{237}Np	322	3609	4.87
					4.87±0.02

Our second objective was to define the uncertainty involved in the time required for inserting and removing the samples from the reactor. The irradiation times for the tests discussed above were too long (~1 hr) to get an accurate measure of this uncertainty; therefore, we irradiated two ^{237}Np samples (7-1 and 7-2) for 6 min each in separate irradiations that yielded about 15,000 tracks per exposure. In this case, the deviation between the two samples was 1.85%. We estimate that roughly 1% is due to uncertainties in insertion and removal times; this corresponds to an uncertainty of about 10 sec. Thus, for a 1-hr exposure this uncertainty is negligible.

2. Reaction-Rate Measurements in CFRMF By Foil Activation

Two irradiations of dosimetry foils were conducted in CFRMF. A preliminary, low-power test was run on December 6, 1971 for 7 hr at a nominal reactor power level of 0.6 kW, and a higher-power test was run for 7 hr at 9.75 kW on February 15, 1972. The low-power test included ^{235}U foils as well as the SSTR samples previously discussed. The high-power test included primarily nonfissile foils used for dosimetry purposes; however, ^{235}U and ^{238}U foils were also included. Table 6 tabulates the results from the latter test. Two items were of particular interest in these tests: (1) the reliability of various fission-product yields which we had previously measured in the ZPR-3 mockup critical experiments[14] and (2) comparison of fission-rate results from the three methods used in CFRMF namely, foil-activation, SSTR, and fission-chamber measurements.

Table 7 summarizes the fission-rates obtained for ^{235}U and ^{238}U in the high-power test, which are based upon individual fission-product measurements. The fission yields in this table are our previously reported values.[14] The fission rates as determined from the individual fission products (except ^{131}I) are quite consistent. The standard deviation of the individual fission rates from the average rate is 1.0% for ^{235}U and 2.2% for ^{238}U; the standard error in the fission rate as determined from a single fission product is 2.1% for ^{235}U and 4.4% for ^{238}U. These uncertainties are less than the errors assigned to the fission-yield measurements previously reported.

TABLE 6. Summary of Measured Reaction Rates for ANL-1 Foil Set

Reaction	Sample Number	Type of Detector	Times Counted	Relative Precision, %	Gamma-Ray Self Absorption	Reaction Rate ($\bar{\sigma}\phi$), 10^{-15} atoms/(atom)(sec)	1σ Absolute Error, %
$^{27}Al(n,\alpha)^{24}Na$	6	NaI	3	0.3	1.00	0.0209	5.8
	5	NaI	2	0.1	1.00	0.0206	5.8
	4	NaI	3	0.5	1.00	0.0209	5.8
	2	Ge(Li)	4	0.8	0.998	0.0206	5.5
$^{197}Au(n,\gamma)^{198}Au$	4	Ge(Li)	4	0.2	1.00	53.3	2.4
	2	Ge(Li)	3	0.3	1.00	54.2	2.4
	3	Ge(Li)	4	0.2	1.00	52.8	2.4
	2	Ge(Li)	4	0.6	0.996	54.2	2.5
$^{115}In(n,n')^{115m}In$	6	NaI,Ge(Li)	2	0.8	0.998	6.33	3.2
	5	NaI,Ge(Li)	2	0.8	0.998	6.36	3.2
	4	NaI,Ge(Li)	3	0.7	0.998	6.36	3.2
$^{59}Co(n,\gamma)^{60}Co$	6	Ge(Li)	4	0.5	1.00	9.37	2.4
	5	Ge(Li)	4	0.3	1.00	8.49	2.4
	4	Ge(Li)	4	0.2	1.00	9.01	2.5
$^{58}Ni(n,p)^{58}Co$	TE	Ge(Li)	3	0.3	0.992	3.07	5.5
$^{54}Fe(n,p)^{54}Mn$	B	Ge(Li)	5	1.0	0.978	2.21	2.7
$^{54}Fe(n,\alpha)^{51}Cr$	B	Ge(Li)	5	3.3	0.966	0.0292	6.4
$^{58}Fe(n,\gamma)^{59}Fe$	B	Ge(Li)	4	0.5	0.981	0.753	3.0
$^{46}Ti(n,p)^{46}Sc$	P	Ge(Li)	4	0.2	0.996	0.340	2.4
	O	Ge(Li)	6	1.0	0.996	0.337	2.6
$^{47}Ti(n,p)^{47}Sc$	P	Ge(Li)	6	0.8	0.990	0.542	5.5
	O	Ge(Li)	6	0.5	0.990	0.547	5.5
$^{48}Ti(n,p)^{48}Sc$	P	Ge(Li)	7	1.0	0.996	0.00857	5.6
	O	Ge(Li)	8	0.6	0.996	0.00861	5.5
$^{45}Sc(n,\gamma)^{46}Sc$	2	Ge(Li)	6	0.3	0.999	2.94	2.4
$^{238}U(n,\gamma)^{239}Np$	2	Ge(Li)	5	0.8	0.985	22.5	5.5
$^{235}U(n,f)^{140}Ba$	2	Ge(Li)	6	0.4	0.994	212.6	4.3
$^{238}U(n,f)^{140}Ba$	2	Ge(Li)	5	0.8	0.999	9.99	4.4

TABLE 7. Fission-Product Reaction Rates for ^{235}U and ^{238}U

Fission Product	^{235}U Reaction Rate $\times 10^{14}$	^{235}U Error, % Relative	^{235}U Error, % Absolute	^{235}U Fission Yield, %	^{235}U Fission Rate $\times 10^{13}$	^{238}U Reaction Rate $\times 10^{16}$	^{238}U Error, % Relative	^{238}U Error, % Absolute	^{238}U Fission Yield, %	^{238}U Fission Rate $\times 10^{15}$
^{95}Zr	1.33	0.9	3.1	6.41	2.08	5.09	0.7	3.1	5.44	9.35
^{103}Ru	0.680	0.3	2.4	3.29	2.06	6.33	0.2	2.4	6.29	10.07
^{131}I	0.640	1.1	2.7	3.44	1.86	3.11	0.9	2.6	3.64	8.54
^{132}Te	0.962	1.0	3.9	4.77	2.01	5.64	1.2	3.9	5.35	10.5
^{140}Ba	1.22	0.4	2.5	5.80	2.10	5.82	0.8	2.6	5.90	9.87
					2.06±0.02					9.95±0.22

Next we consider the question of absolute accuracy of ^{235}U fission-rate determinations in CFRMF. Fission rates for ^{235}U, ^{237}Np, ^{239}Pu, and ^{238}U were measured by fission chambers[15] at a nominal reactor-power level of 0.6 kW; we have SSTR and foil activation rate results for ^{235}U at the same reactor power level. With the assumption that all measurements were indeed at the same power level, we find that for ^{235}U the SSTR results are 2.5% higher than the fission-chamber results, and 0.8% higher than the activation-rate results. At this stage, it is difficult to relate the activation-rate results measured at 9.75 kW to the SSTR data measured at 0.6 kW because of questions relating to the absolute power normalization. If, however, we assume that the stated reactor-power levels are correct, we find that the SSTR results are 1.9% higher than the activation-rate results. In summary, a preliminary analysis of the data suggests that all three methods for measuring ^{235}U fission rates are consistent within 2 to 3%; thus, we are approaching the objective of 1.5% (1σ) accuracy.

A comparison of ^{237}Np fission rates measured by SSTR and by fission chambers shows a discrepancy of 7.5% between the results. The source of this discrepancy has not been identified, but the most probable cause is the weights of materials on the SSTRs and/or the fission-chamber foils. Foil-activation measurements, which are to be made soon, may help to identify the source of the discrepancy.

B. Service Dosimetry

(R. R. Heinrich, N. D. Dudey)

This program is devoted to providing fast-neutron dosimetry measurements for all ANL programs and to coordinating ANL's overall dosimetry efforts. At present, our capabilities include designing the dosimetry aspects of fast-neutron irradiation experiments, measuring reaction rates from the dosimetry monitors, and determining flux and fluence from the reaction-rate data. In the near future, we will have the capability for determining neutron spectra, the number of atomic displacements produced in a fast-neutron irradiation, and the burnup of a fuel sample; all of these data will be derived from the basic dosimetry measurements.

A series of EBR-II dosimetry tests conducted at both low [50 kW(t)] and high reactor power [62.5 MW(t)] has recently been completed. The purpose of these tests was to characterize the neutronic parameters of fission rate, neutron flux, and neutron spectrum for the reactor under operating conditions of 62.5 MW(t) power level, a uranium radial reflector, and a stainless steel axial reflector. Although these neutronic parameters can be calculated using sophisticated two-dimensional, multienergy-group computer codes, the confidence placed on the calculational techniques depends significantly upon experimental confirmation. For this reason dosimetry measurements were considered essential to confirm these calculational techniques; moreover, they have provided a sound basis for the design and analysis of future irradiations.

These dosimetry measurements were part of a coordinated program undertaken by the EBR-II Project of ANL and the Irradiation Analysis Section of The Hanford Engineering Development Laboratory (HEDL). The emphasis of the HEDL program was to obtain empirical data on neutron reaction rates of a variety of materials, from which full-power neutron spectra and fluence could

be deduced at the point of measurement, and to extend similar measurements made in Run 31F, an earlier EBR-II dosimetry study. The ANL emphasis was to provide benchmark measurements that would substantiate and refine neutronics calculations at low and high power.

This series of tests has extended earlier flux-characterization measurements obtained in Runs 29, 31F, and 46 to other regions of the reactor core and blanket and has permitted the examination of neutronic-parameter changes in both high- and low-density structural subassemblies. The tests were made in three reactor operating runs, each with identical reactor loadings. The first irradiation (Run 50G) and the third (Run 51B) were conducted at 50 kW(t) for a period of 1 hr and emphasized measurements of ^{235}U and ^{238}U relative fission-rate distributions, both axially and radially throughout the reactor. However, additional dosimetry packets containing fissile and nonfissile materials were placed at selected positions for the determination of absolute activation rates. The second irradiation (Run 50H) was conducted at a constant power of 62.5 MW(t) over a period of 209 hr and contained a large number of fissile and nonfissile dosimetry foils. These dosimeters were predominantly located in structural-type subassemblies, but a few were also included in driver subassemblies.

The basic dosimetry packets contained foil sets of ^{235}U, ^{238}U, ^{237}Np, ^{239}Pu, ^{197}Au, and ^{58}Ni. Fissile monitors were prepared and encapsulated in vanadium by Oak Ridge National Laboratory. Additional monitors of Al, Sc, Ti, Fe, Co, Cu, and Ag were included with the basic set in structural subassemblies at several reactor positions. The vanadium-encapsulated fissile foils were placed in the tube-like enclosures, whereas the nonfissile foils were primarily in the structural form of thin washers. The total number of dosimeter foils included in the three irradiations was nearly 5000. Of the fissile and activation foils, about 50% of these were analyzed by HEDL and 25% each by ANL-West and this group. Samples from each of the three irradiations were exchanged between the two participating ANL groups, and a round-robin exchange of selected sample sets irradiated at high power was also conducted by all three laboratories.

Counting of the samples in this laboratory was primarily done by Ge(Li) gamma spectrometry, although some of the individual gamma-ray activation products, such as ^{198}Au and ^{58}Co, were counted on a NaI(Tl) detector. Calibration of the detectors was performed by the use of absolute standards covering the gamma-energy range of the dosimetry samples. Although this calibration technique is a standard procedure, it did require an extension in distance beyond the normal counting positions because of the high activity level of the samples irradiated in the high-power tests. These samples were counted at calibrated positions of 200 and 400 cm, whereas the samples irradiated in the low-power tests were counted at a more normal position of 10 cm. Counting data for the reaction products from the activation foils and the fission products ^{95}Zr, ^{103}Ru, ^{131}I, ^{132}Te, and ^{140}La from the fissile foils were reported to the EBR-II Project in units of dps/mg and atoms/(atom)(sec) at time zero. Appropriate corrections had been made to the data for Compton scattering, air absorption, capsule absorption, self-absorption, and saturated activity.

Initial comparisons of results among HEDL, ANL-West, and this group revealed significant discrepancies. These discrepancies were associated with the samples having the highest activity levels. The source of the problem was subsequently identified as random summing of pulses in the detection electronics. Random summing can be briefly described as follows: pulses arriving in the amplifier portion of the electronic system within a time τ are removed from their respective energy values to give the appearance of a single higher-energy pulse. Our studies indicated that τ is of the order of 4 to 7 μsec, with the result that, at detector counting rates of 5×10^3 cps, the loss of pulses is ∿3%, and at 1×10^4 cps, about 6%. Further measurements at each laboratory revealed that this effect indeed quantitatively accounted for the observed discrepancies.

Reevaluation of our data showed that corrections of less than 1% were required, except for one sample which required a 3% correction. However, data reported by the other laboratories required corrections that were typically 5 to 6% and in some cases as large as 15%. ANL-West has now recounted their samples and the corrected data are in substantial agreement with our data. Revision of the data from HEDL has not been completed; however, on the basis of the corrected ANL-West results, the overall agreement is expected to be better than 3%.

Very preliminary analysis of our results from this study has begun. This analysis has primarily been concerned with ascertaining the reliability of the data. The first test was to examine the applicability of the fission yields[14] used in the analysis. The method was similar to that described in the preceding section for fission-rate measurements in CFRMF. If $(\sigma_i \phi)$ is the measured-fission product reaction rate for the ith fission product, then the fission rate based upon the ith fission product is:

$$(\sigma_f \phi)_i = \frac{(\sigma_i \phi)}{(FY)_i}$$

where $(FY)_i$ is the fission yield for the fission product. Fission rate ratios are then a convenient means for identifying computational errors and for examining the precision of both the measured reaction rates and fission yields. The nuclide ^{140}Ba was chosen as the reference fission product because its yield is the only fast-neutron yield available for fast fission of ^{237}Np.

Ratios of the type $(\sigma_f \phi)_i / (\sigma_f \phi)_{Ba}$ were computed for 15 samples of ^{235}U and 15 samples of ^{238}U from the low-power [15 kW(t)] test and for about 20 samples each of ^{235}U, ^{238}U, and ^{239}Pu from the high-power [62.5 MW(t)] test. For a given fissionable material, the mean value of each ratio indicates the relative accuracy of the fission yields, and the standard error indicates the precision of a single reaction-rate measurement. Table 8 summarizes the results of this analysis. From these data, we have drawn the following conclusions:

1. The data for ^{131}I are inconsistent with the data for other fission products, i.e., the fission rates based on ^{131}I are lower than those based on other fission products. This inconsistency, which was also observed in the CFRMF tests, suggests that the ^{131}I yields previously reported[14] may be too large. Moreover, the fission rates based upon ^{131}I show a greater

TABLE 8. Ratios of Fission Rates Measured By Selected Fission Products and ^{140}Ba

Fissile Nuclide	Fission Product i	Fission Rate Ratio, $(\sigma_f\phi)_i/(\sigma_f\phi)_{^{140}Ba}$ Low-Power Test (50 kW)	High-Power Test (62.5 MW)
^{235}U	^{103}Ru	0.98 ± 0.02	0.92 ± 0.02
	^{95}Zr	0.98 ± 0.01	0.94 ± 0.03
	^{131}I	0.93 ± 0.04	0.86 ± 0.06
^{238}U	^{103}Ru	1.02 ± 0.06	0.99 ± 0.03
	^{95}Zr	1.00 ± 0.02	0.98 ± 0.03
	^{131}I	0.87 ± 0.02	0.79 ± 0.04
^{239}Pu	^{103}Ru	-	0.97 ± 0.02
	^{95}Zr	-	0.99 ± 0.03
	^{131}I	-	0.78 ± 0.03

negative deviation in the high-power test than in the low-power test. These findings suggest the possibility that iodine is being lost from the foil samples by virtue if its volatility and/or mobility. If this is the case, iodine would not be a reliable fission-rate monitor.

2. With the exception of the ^{235}U measurement at high power, the fission rates determined from ^{95}Zr, ^{103}Ru, and ^{140}Ba are consistent within ±3%. This implies that any of these nuclides may be used as accurate fission rate monitors in EBR-II and that the fission yields used in these tests are probably accurate to 2-3%.

3. The standard deviations for all ratios are less than 1%, thus implying a high degree of confidence in the fission-product reaction-rate data.

4. A real discrepancy (outside of statistical expectations) exists between ^{235}U fission-rate results from the low- and high-power tests. This observation is quite surprising and as yet is unexplainable. We find that ^{235}U fission rates determined from ^{103}Ru and ^{95}Zr are self-consistent between the low- and high-power tests, yet fission rates based upon ^{140}Ba appear to differ by 6-8% between high and low power. It must be pointed out that the fission yields applied here were, in fact, measured in low-power experiments.[14] This apparent problem could be quite important to fast-reactor dosimetry and is presently being investigated further.

APPENDIX A

Evaluations have been made of the available cross-section data for the reactions $^{56}Fe(n,p)^{56}Mn$ and $^{32}S(n,p)^{32}P$. These studies were conducted as part of the effort by the Normalization and Standards Subcommittee of the Cross Sections Evaluation Working Group of the Division of Reactor Development Technology of the AEC to standardize cross-section data used for neutron dosimetry purposes. The evaluations that we presented to the Working Group are given below.

1. Revised Evaluation of the $^{56}Fe(n,p)^{56}Mn$ Cross Section

The literature examined in this review includes all references to cross-section measurements of the $^{56}Fe(n,p)^{56}Mn$ reaction that are listed in CINDA 71 and its supplements, plus some very recent measurements near the reaction threshold. Data for the neutron-energy range from threshold (2.971 MeV) to 20 MeV were considered. This evaluation is a revision of the preliminary version which was presented to the Working Group on March 29, 1972. The two major revisions are that (1) all reference cross sections have been renormalized to ENDF/B, Version 3 cross sections, and (2) weighted least-squares fitting routines were used to systematize the evaluations.

Virtually all measurements of the $^{56}Fe(n,p)^{56}Mn$ reaction were made by measuring ^{56}Mn in activated natural iron samples. As a result, the contributions of ^{56}Mn from the $^{57}Fe(n,np+d)$ and $^{58}Fe(n,t)$ reactions are included in the measurements. For dosimetry purposes, elemental iron is usually used; therefore, the evaluated cross sections are appropriate for this application. However, it should be recognized that this evaluation is not strictly limited to the $^{56}Fe(n,p)$ reaction. For example, Chittenden[16] measured the $^{57}Fe(n,np)$ cross section at 14.8 MeV and obtained a value of 6.1 mb. Considering the isotopic abundances of ^{56}Fe and ^{57}Fe, the $^{57}Fe(n,np)^{56}Fe$ reaction contributes less than 0.3% to the ^{56}Fe activity at 14.8 MeV. Above 15 MeV, the interfering reaction may be more significant.

Our approach to this evaluation was largely based upon a subjective analysis of the experimental techniques. From this analysis, we assigned a weighting factor to each of the reported results. Because many measurements were made relative to other reaction cross sections, it was necessary to renormalize the reference cross sections in a self-consistent manner. This was accomplished by renormalizing all reference and monitor cross sections to the ENDF/B, Version 3 data sets. Santry and Butler[17] measured the $^{56}Fe(n,p)$ reaction relative to the $^{32}S(n,p)$ reaction. As a result, it was necessary to evaluate the $^{32}S(n,p)$ reaction, since it is not included in ENDF/B. Our evaluation of $^{32}S(n,p)$, which is presented in the following subsection, was used to renormalize the Santry and Butler $^{56}Fe(n,p)$ data. Liskien and Paulsen[18] measured their data relative to $H(n,p)$ and no renormalization was considered necessary. Both Grundl[19] and Meadows[20] measured $^{56}Fe(n,p)$ relative to $^{238}U(n,f)$; therefore, both data sets were renormalized to ENDF/B $^{238}U(n,f)$ values. Cuzzocrea and Perillo[21] report a number of measurements for $^{56}Fe(n,p)$ and several other cross sections, including $^{27}Al(n,\alpha)$ between 13.7 and 14.7 MeV. In general, all of their results appear high. For these data, we assumed a flux-calibration problem and renormalized their ^{56}Fe data by relating their $^{27}Al(n,\alpha)$ results to the revised evaluation of ^{27}Al prepared by P. G. Young.[22] Hemingway[23] reported ^{56}Fe results by the associated particle technique; therefore, no renormalization was necessary.

Fourteen individual measurements[24-38] are reported for the energy region 14 to 15 MeV. These data were weighted according to our assessment and a best fit in this energy region was calculated. Bormann[38] and Terrell and Holm[39] report ^{56}Fe cross sections normalized to ^{56}Fe values of 112.5 mb at 14.1 MeV and 110 mb at 14.3 MeV, respectively. From our fitted curve, we renormalized Bormann's results to a value of 110.3 mb and Terrell and Holm's to a value of 108.8 mb, at the respective energies.

Bresesti[40] and Fabry[41] measured a number of spectrum-averaged cross section ratios in a thermal-neutron-induced ^{235}U fission spectrum. Bresesti assumed a cross-section shape for ^{56}Fe based upon Liskien-Paulsen[18] and Santry-Butler[17] and determined the magnitude based upon integral ratios and an assumed fission spectrum. Fabry did essestially the same, except that he allowed the shapes to vary in an ill-defined way to measure ^{56}Fe relative to six other cross sections including $^{235}U(n,f)$. We have chosen to adjust Fabry's ^{56}Fe data by renormalizing his reported ^{235}U (n,f) data to the ENDF/B-3 evaluation.

Finally, all renormalized cross sections were weighted according to our subjective analysis and the data were fit by the least-squares method to obtain our evaluated excitation function. Figures A1 and A2 show all the renormalized data together with our evaluated curve. The evaluated cross sections are tabulated in Table A1 in the ENDF/B format, using an energy grid such that a linear interpolation between points will result in a negligible error. Figure A3 shows a comparison of our evaluation with those of Kanda and Nakasima[42] and the SAND-II evaluated library.[43] All three evaluations are very similar up to about 15 MeV, where SAND-II begins to deviate significantly.

We feel, on the basis of this evaluation, that the shape of the excitation function is established with considerable confidence and that the magnitudes of the cross sections are established to within about ±5%. For dosimetry applications to LMFBR-type neutron spectra, no further experimental work seems to be necessary.

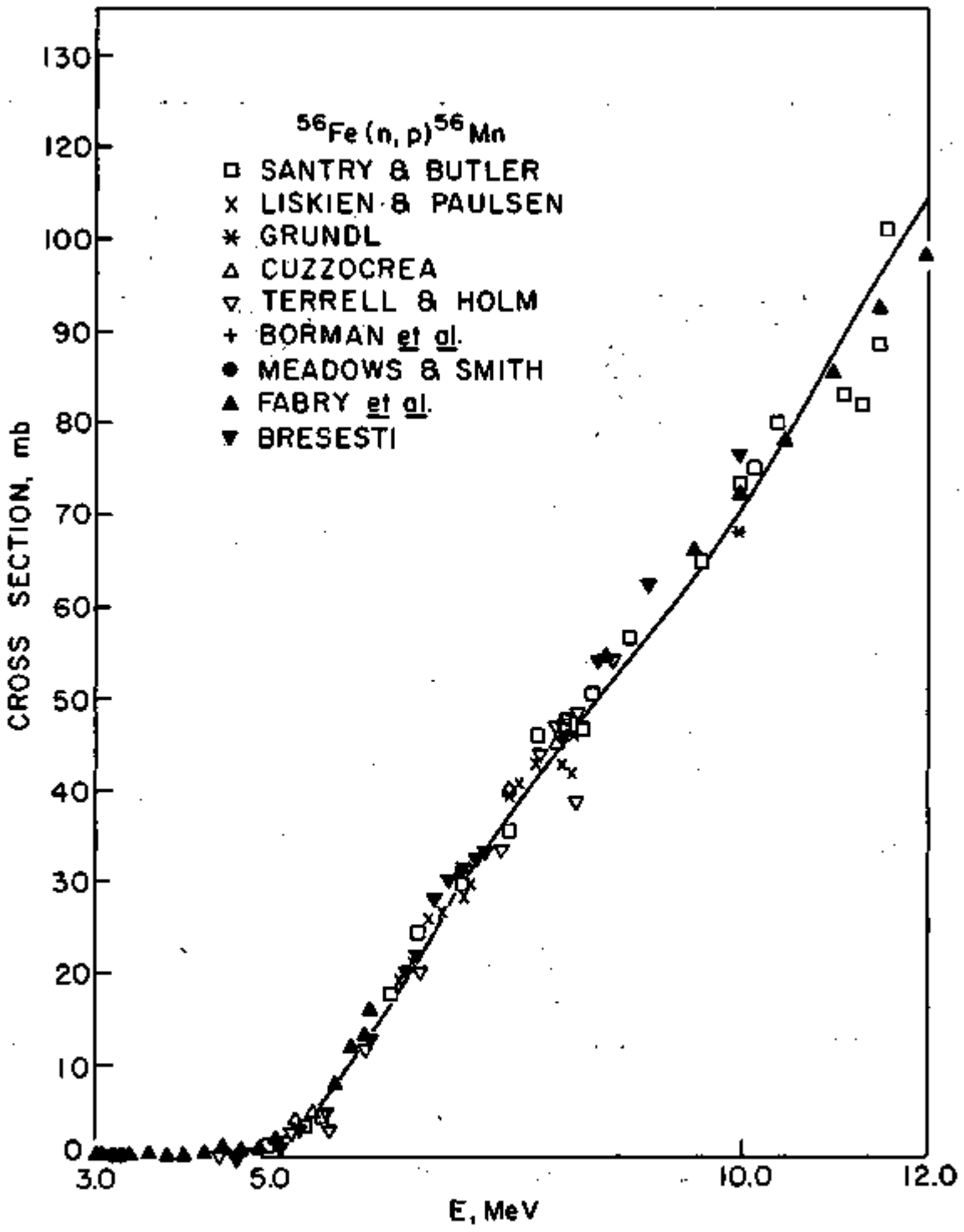

Fig. A1. Cross-Section Data for ^{56}Fe(n,p)^{56}Mn at Neutron Energies from 3.0 to 12.0 MeV.

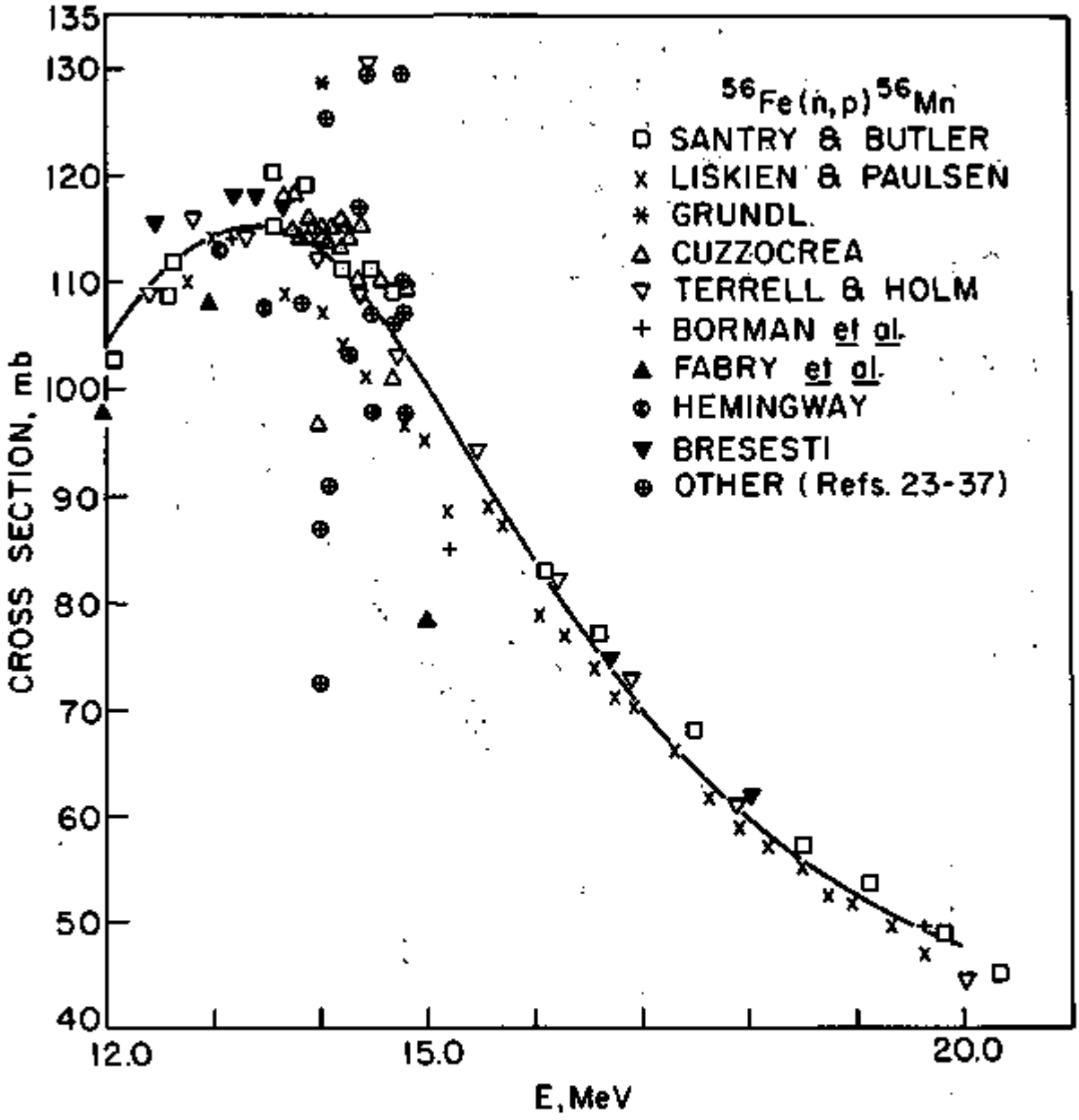

Fig. A2. Cross-Section Data for $^{56}Fe(n,p)^{56}Mn$ at Neutron Energies from 12.0 to 20.0 MeV

TABLE A1. Evaluated Cross-Section Data for the $^{56}Fe(n,p)^{56}Mn$ Reaction Tabulated in ENDF/B Format

Energy, ev	Sigma, b	Energy, ev	Sigma, b	Energy, ev	Sigma, b
2.97000+ 6	0.00000+ 0	3.00000+ 6	1.10000- 7	3.10000+ 6	1.50000- 7
3.20000+ 6	2.10000- 7	3.30000+ 6	2.95000- 7	3.40000+ 6	4.20000- 7
3.50000+ 6	6.20000- 7	3.60000+ 6	9.80000- 7	3.70000+ 6	1.50000- 6
3.80000+ 6	2.50000- 6	3.90000+ 6	4.40000- 6	4.00000+ 6	8.00000- 6
4.10000+ 6	1.20000- 5	4.20000+ 6	2.90000- 5	4.30000+ 6	5.60000- 5
4.40000+ 6	9.30000- 5	4.50000+ 6	1.50000- 4	4.60000+ 6	2.38000- 4
4.70000+ 6	3.75000- 4	4.80000+ 6	5.55000- 4	4.90000+ 6	8.80000- 4
5.00000+ 6	1.23000- 3	5.10000+ 6	1.70000- 3	5.20000+ 6	2.14000- 3
5.30000+ 6	3.28000- 3	5.40000+ 6	4.50000- 3	5.50000+ 6	5.80000- 3
5.60000+ 6	7.16000- 3	5.80000+ 6	1.01000- 2	6.00000+ 6	1.32000- 2
6.20000+ 6	1.64000- 2	6.40000+ 6	1.98000- 2	6.60000+ 6	2.31000- 2
6.80000+ 6	2.64000- 2	7.00000+ 6	2.96000- 2	7.50000+ 6	3.72000- 2
8.00000+ 6	4.40000- 2	8.50000+ 6	5.04000- 2	9.00000+ 6	5.67000- 2
9.50000+ 6	6.33000- 2	1.00000+ 7	7.06000- 2	1.05000+ 7	7.87000- 2
1.10000+ 7	8.72000- 2	1.15000+ 7	9.56000- 2	1.20000+ 7	1.03000- 1
1.22000+ 7	1.06000- 1	1.24000+ 7	1.08000- 1	1.26000+ 7	1.10000- 1
1.28000+ 7	1.12000- 1	1.30000+ 7	1.13000- 1	1.31000+ 7	1.13000- 1
1.32000+ 7	1.14000- 1	1.33000+ 7	1.14000- 1	1.34000+ 7	1.14000- 1
1.35000+ 7	1.14000- 1	1.36000+ 7	1.13000- 1	1.38000+ 7	1.13000- 1
1.39000+ 7	1.12000- 1	1.41000+ 7	1.11000- 1	1.42000+ 7	1.10000- 1
1.43000+ 7	1.09000- 1	1.44000+ 7	1.08000- 1	1.45000+ 7	1.07000- 1
1.46000+ 7	1.04000- 1	1.47000+ 7	1.04000- 1	1.48000+ 7	1.02000- 1
1.49000+ 7	1.01000- 1	1.50000+ 7	9.94000- 2	1.55000+ 7	9.07000- 2
1.60000+ 7	8.18000- 2	1.65000+ 7	7.62000- 2	1.70000+ 7	6.92000- 2
1.75000+ 7	6.35000- 2	1.80000+ 7	5.89000- 2	1.85000+ 7	5.47000- 2
1.90000+ 7	5.13000- 2	1.95000+ 7	4.92000- 2		

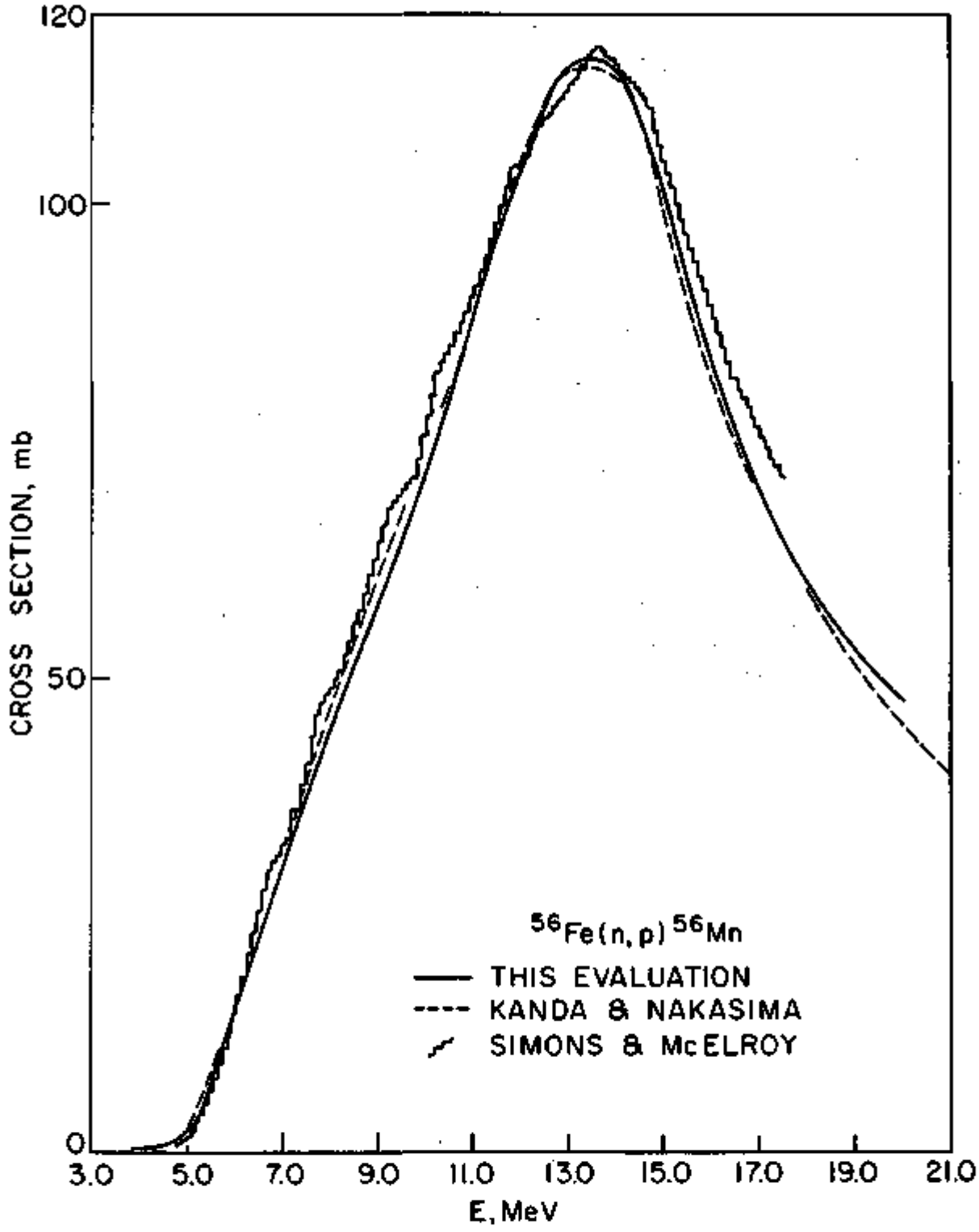

Fig. A3. Evaluations of Cross-Section Data for $^{56}Fe(n,p)^{56}Mn$

2. Evaluation of the $^{32}S(n,p)^{32}P$ Reaction

The literature examined in this review includes all references in CINDA 71 and its supplements. Four sets of data have been reported for $^{32}S(n,p)$ cross sections between the reaction threshold (∿0.956 MeV) and 5 MeV.[44-47] All investigators used the activation technique and measured cross sections relative to a flux monitor. The principal uncertainty in these four sets of data appears to be in beta counting of the sulfur pellets because of self absorption and self-scattering of beta particles in the relatively thick sulfur targets.

The four data sets are shown in Fig. A4. Klema and Hansen[44] used a uranium fission chamber as a flux monitor in measuring the $^{32}S(n,p)$ cross sections. Neither the isotopic composition nor the uranium cross sections that they used for their analysis was reported; therefore, it is not possible to renormalize their results to a self-consistent set of reference cross sections based on ENDF/B-3. Lüscher[45] measured the ^{32}S cross sections on a relative basis and then normalized to the data of Klema and Hansen.[44] Hürlimann and Huber[46] calibrated a Hornyach detector relative to H(n,p) and then measured $^{32}S(n,p)$ relative to the calibrated detector. Allan et al.[47] measured ^{32}S using a ^{238}U fission chamber as a flux monitor; we have renormalized their data to the ENDF/B-3 $^{238}U(n,f)$ cross sections. The structure in the cross-section data between 1.6 MeV and ∿5 MeV is well reproduced by both Lüscher[45] and Hürlimann-Huber[46] except for a 20-50 keV difference in the neutron energy scale. We have chosen to increase the neutron energies of the Hürlimann-Huber data by 20 keV between 2.2 and 2.9 MeV and by 50 keV for data at energies higher than 3.0 MeV. The data presented in Fig. A4 show the reported energies before our energy adjustment. With the exception of the measurements in the energy region between 2.25 and 2.55 MeV, the agreement between the four experiments is reasonably good. After renormalization, the data of Allen et al.[47] agree well with those of Klema and Hanson[44] from 3.4 to 5.8 MeV.

The cross-section data for neutron energies between 5.0 and 20.3 MeV are presented in Fig. A5. From 5.8 to 9.6 MeV, data are available only from Allen et al. From 10.4 to 11.6 MeV, Santry and Butler[48] have measured ^{32}S on a relative basis and normalized to the data of Allen et al. at lower energy. We have renormalized the Santry-Butler values relative to the renormalizated Allen data. From 13 to 15 MeV, Allen et al. measured the ^{32}S cross section on an absolute basis by the associative particle technique. Santry and Butler[48] measured the ^{32}S cross section from 12.5 to 20.3 MeV on a relative basis and normalized to the results of Allen et al. at 14.50 MeV. Both measurements seem acceptable without any renormalization. Between 14.0 and 14.8 MeV, eight individual $^{32}S(n,p)$ cross section measurements are reported.[49-56] These data, which are given in Fig. A5 with error bars indicated, show considerable scatter but a fitted curve through these values is not too different from the data of either Allen et al.[47] or Santry-Butler.[48]

The evaluated cross sections are shown as the solid lines in Figs. A4 and A5. Below 5 MeV the evaluation was based upon a "best" curve through the available data. In arriving at the curve, we adjusted the energy scale of the Hürlimann-Huber data by 20 keV between 2.2 and 2.9 MeV and by 50 keV for data greater than 3.0 MeV. (This adjustment is not reflected in their data as presented in Fig. A4.) With this adjustment, all of the data were in good agreement and a "best" fit curve was used. From 5 to 14

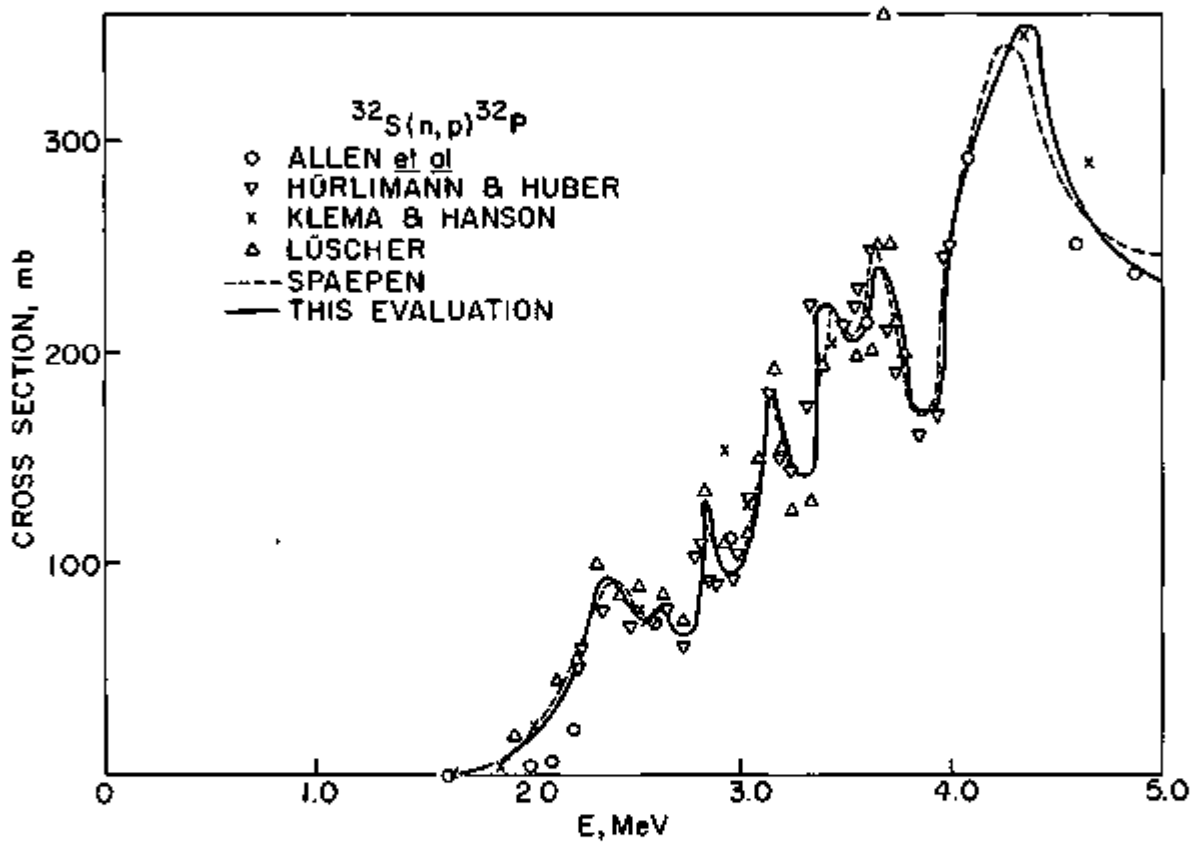

Fig. A4. Cross-Section Data for $^{32}S(n,p)^{32}P$ for Neutron Energies from 1.6 to 5.0 MeV

MeV the adjusted data of Allen et al.[47] were used for the evaluation. Between 14 and 14.8 MeV, a least squares fit to all available data, weighted according to our assessment of the quality of data, was used. Above 15 MeV, our evaluation follows the Santry-Butler[48] data. An evaluation by Spaepen[57] is shown in Figs. A4 and A5 for comparison purposes. Our overall evaluation is also tabulated in Table A2 in the ENDF/B format.

Because $^{32}S(n,p)$ has been extensively used as a cross-section reference reaction, we feel that additional measurements from threshold to 20 MeV are desirable. We have concluded from our evaluation that the cross sections for $^{32}S(n,p)$ are not sufficiently established for use of this reaction as a reference standard.

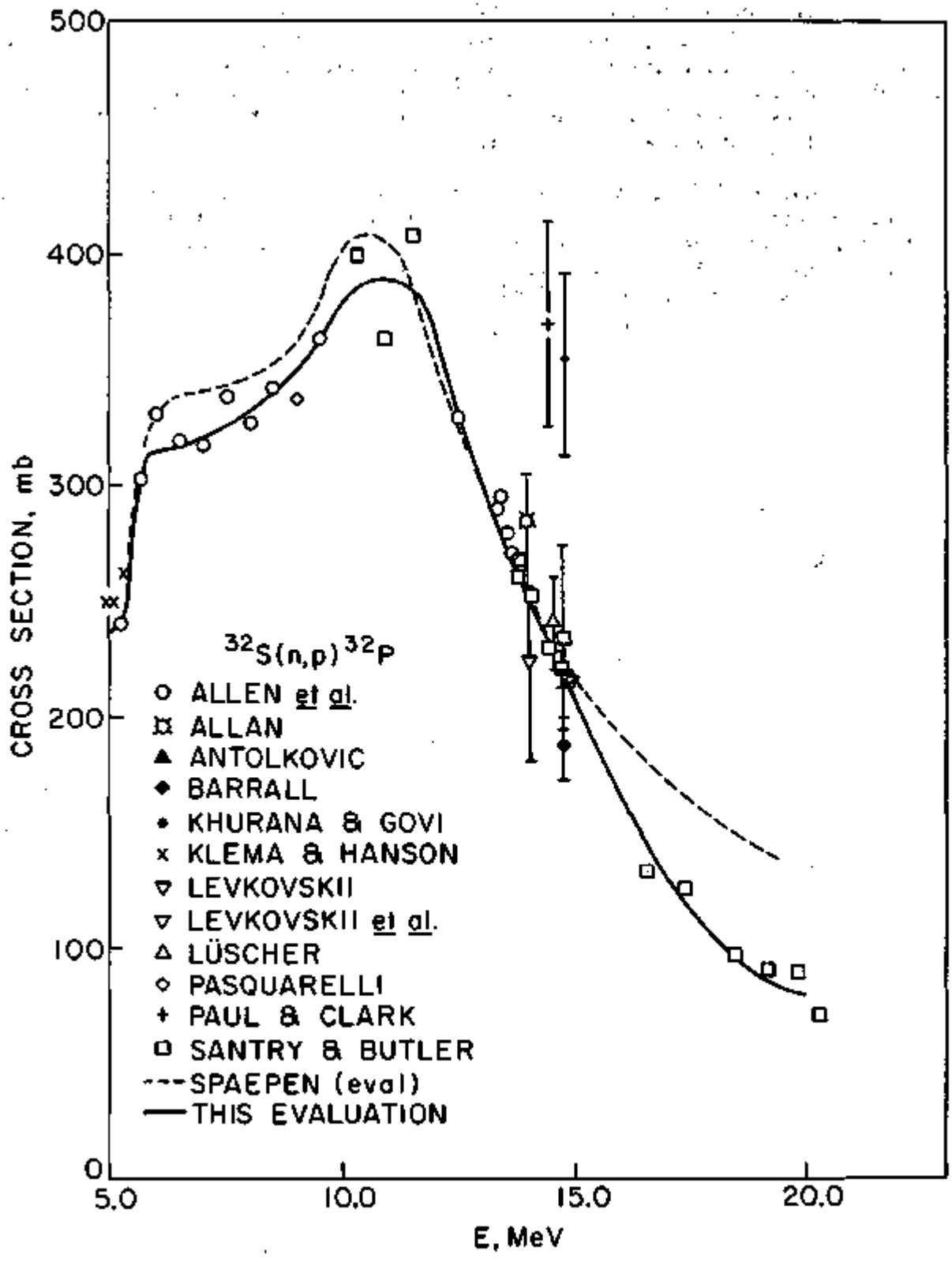

Fig. A5. Cross-Section Data for $^{32}S(n,p)^{32}P$ for Neutron Energies from 5.0 to 20.3 MeV

TABLE A2. Evaluated Cross-Section Data for the $^{32}S(n,p)^{32}P$ Reaction Tabulated in ENDF/B Format

Energy, ev	Sigma, b	Energy, ev	Sigma, b	Energy, ev	Sigma, b
9.57000+ 5	0.00000+ 0	1.00000+ 6	1.28000- 5	1.10000+ 6	2.50000- 5
1.20000+ 6	5.00000- 5	1.30000+ 6	1.12000- 4	1.40000+ 6	2.30000- 4
1.50000+ 6	4.70000- 4	1.60000+ 6	9.50000- 4	1.70000+ 6	1.80000- 3
1.80000+ 6	4.00000- 3	1.90000+ 6	7.80000- 3	2.00000+ 6	1.45000- 2
2.10000+ 6	2.95000- 2	2.20000+ 6	5.20000- 2	2.30000+ 6	8.40000- 2
2.35000+ 6	9.40000- 2	2.40000+ 6	8.65000- 2	2.50000+ 6	7.30000- 2
2.60000+ 6	7.90000- 2	2.70000+ 6	6.60000- 2	2.80000+ 6	1.29000- 1
2.90000+ 6	9.30000- 2	3.00000+ 6	1.29000- 1	3.10000+ 6	1.82000- 1
3.20000+ 6	1.41000- 1	3.25000+ 6	1.35000- 1	3.30000+ 6	1.88000- 1
3.35000+ 6	2.23000- 1	3.40000+ 6	2.10000- 1	3.45000+ 6	2.01000- 1
3.50000+ 6	2.02000- 1	3.60000+ 6	2.38000- 1	3.70000+ 6	2.10000- 1
3.80000+ 6	1.66000- 1	3.90000+ 6	1.85000- 1	4.00000+ 6	2.70000- 1
4.10000+ 6	3.05000- 1	4.20000+ 6	3.34000- 1	4.30000+ 6	3.49000- 1
4.40000+ 6	3.24000- 1	4.60000+ 6	2.54000- 1	4.80000+ 6	2.30000- 1
5.00000+ 6	2.35000- 1	5.20000+ 6	2.35000- 1	5.40000+ 6	2.40000- 1
5.60000+ 6	2.77000- 1	5.80000+ 6	3.03000- 1	6.00000+ 6	3.11000- 1
6.50000+ 6	3.14000- 1	7.00000+ 6	3.16000- 1	7.50000+ 6	3.20000- 1
8.00000+ 6	3.24000- 1	8.50000+ 6	3.30000- 1	9.00000+ 6	3.40000- 1
9.50000+ 6	3.54000- 1	1.00000+ 7	3.70000- 1	1.05000+ 7	3.82000- 1
1.10000+ 7	3.85000- 1	1.15000+ 7	3.84000- 1	1.20000+ 7	3.66000- 1
1.25000+ 7	3.28000- 1	1.30000+ 7	3.08000- 1	1.35000+ 7	2.80000- 1
1.40000+ 7	2.53000- 1	1.45000+ 7	2.25000- 1	1.50000+ 7	2.10000- 1
1.60000+ 7	1.64000- 1	1.70000+ 7	1.27000- 1	1.80000+ 7	1.10000- 1
1.60000+ 7	1.64000- 1	1.70000+ 7	1.27000- 1	1.80000+ 7	1.01000- 1
1.90000+ 7	8.70000- 2	2.00000+ 7	7.70000- 2		

REFERENCES

1. R. G. Nisle and I. E. Stepan, Nucl. Sci. Eng. 39, 257 (1970).

2. S. C. Nilsson, G. Ohlen, C. Gustafson, and P. Moller, Phys. Letters 30B, 437 (1969).

3. Aqueous Processing of LMFBR Fuels--Technical Assessment and Experimental Program Definition, ORNL-4436, Oak Ridge National Laboratory (June 1970).

4. E. L. Albenesius, Phys. Rev. Letters 3, 274 (1959).

5. E. L. Albenesius and R. S. Andrejein, Nucleonics 18(9), 100 (1960).

6. E. N. Sloth, D. L. Horrocks, E. J. Boyce, and M. H. Studier, J. Inorg. Nucl. Chem. 24, 337 (1962).

7. M. Marshall and J. Scobie, Phys. Rev. Letters 23, 583 (1966).

8. N. D. Dudey, Review of Low-Mass Atom Production in Fast Reactors, ANL-7434 (1968).

9. I. Halpern, Ann. Rev. Nucl. Sci. 21, 245 (1971).

10. B. R. Sehgal and R. H. Rempert, Trans. Amer. Nucl. Soc. 14(2), 779 (1971).

11. M. Rajogopalan and T. D. Thomas, Angular Distributions of Alpha Particles Emitted in the Fission of ^{252}Cf, to be published.

12. Z. Fraenkel, Phys. Rev. 154, 1283 (1967).

13. J. R. Nix and W. J. Swiatechi, Nucl. Phys. 71, 1-94 (1965).

14. R. P. Larsen et al., Chemical Engineering Division Burnup, Cross Sections, and Dosimetry Semiannual Report, July-December 1971, ANL-7879, pp. 9-16 (1972).

15. J. Grundl, National Bureau of Standards, private communication (1972).

16. D. M. Chittenden II, D. G. Gardner, and R. W. Fink, Phys. Rev. 122, 860 (1961).

17. D. C. Santry and J. P. Butler, Can. J. Phys. 42, 1030 (1964).

18. H. Liskien and A. Paulsen, J. Nucl. Energy 19, 73 (1965); H. Liskien and A. Paulsen, NUK 8, 315 (1966).

19. J. Grundl, Nucl. Sci. Eng. 40, 331 (1970).

20. J. W. Meadows and D. L. Smith, Argonne National Laboratory, private communication (1972).

21. F. Cuzzocrea and E. Perillo, Nuovo Cimento 54, 53 (1968).

22. P. G. Young, Los Alamos Scientific Laboratory, private communication (1972).

23. J. D. Hemingway, R. H. James, E. B. M. Martin, and G. R. Martin, Proc. Roy. Soc. A292, 180 (1966).

24. D. L. Allan, Nucl. Phys. 24, 274 (1961).

25. G. W. McClure and D. W. Kent, J. Franklin Inst. 260, 238 (1955).

26. H. Pollehn and H. Neuert, Z. Naturforsch. 16A, 227 (1961).

27. R. S. Storey, W. Jack, and A. Ward, Proc. Phys. Soc. (London) 75, 526 (1959).

28. Shinjirō Yasumi, J. Phys. Soc. Japan 12, 443 (1957).

29. S. G. Forbes, Phys. Rev. 88, 1309 (1952).

30. P. Strohal, P. Kulisic, Z. Kolar, and N. Cindro, Phys. Letters 10, 106 (1964).

31. F. Gabbard and B. D. Kern, Phys. Rev. 128, 1276 (1962).

32. W. G. Cross, R. L. Clark, K. Morin, G. Slinn, N. M. Ahmed, and K. Beg. Bull. Amer. Phys. Soc. 7, 335 (1962).

33. E. B. Paul and R. L. Clarke, Can. J. Phys. 31, 267 (1952).

34. G. C. Bonazzola, P. Broretto, E. Chiavassa, R. Spinoglio, and A. Pasquarelli, Nucl. Phys. 51, 337 (1964).

35. R. C. Barrall, M. Silbergeld, and D. G. Gardner, Nucl. Phys. A138, 387 (1969).

36. V. Levkovskii, G. E. Kovel'skaya, G. P. Vinitskaya, V. M. Stepanov, and V. V. Sokol'skii, Soviet J. Nucl. Phys. (English Transl.) 8, 4 (1969).

37. P. Hille, Oesterr. Akad. Wiss. Math. Natrw. Kl. Sitzber. 177, 463 (1969).

38. M. Bormann, S. Cierjacks, R. Lankau, and H. Neuert, Z. Physik 166, 477 (1962).

39. J. Terrell and D. M. Holm, Phys. Rev. 109, 2031 (1958).

40. A. M. Bresesti, M Bresesti, A. Rota, R. A. Rydin, and L. Lesca, Nucl. Sci. Eng. 40, 331 (1970).

41. A. Fabry, M. DeCoster, G. Minsart, J. C. Shepers, and P. Vandeplas, IAEA-CN-26/39, p. 533, Helsinki (1970).

42. Y. Kanda and R. Nakasima, Nat. Bur. Std. Special Publication 299, Vol. 1, p. 193, Washington, D.C. (1968).

43. R. L. Simons and W. N. McElroy, Evaluated Reference Cross Section Library, BNWL-1312 (1970).

44. E. D. Klema and A. O. Hansen, Phys. Rev. 73 (2), 106-110 (1948).

45. E. Lüscher, R. Ricamo, P. Scherrer, and W. Zunt, Helv. Phys. Acta 23, 561-566 (1950).

46. T. Hürlimann and P. Huber, Helv. Phys. Acta 28, 33 (1955).

47. L. Allen, Jr., W. A. Biggers, R. J. Prestwood, and R. K. Smith, Phys. Rev. 107, 1363-1366 (1957).

48. D. C. Santry and J. P. Butler, Can. J. Chem. 41, 123-133 (1963).

49. D. L Allan, Nucl. Phys. 24, 274-299 (1961).

50. B. Antolkovic, Nucl. Phys. 44, 123-129 (1963).

51. R. C. Barrall, M. Silbergeld, and D. G. Gardner, Nucl. Phys. A138, 387-391 (1969).

52. C. S. Khurana and I. M. Govil, Nucl. Phys. 69, 153-157 (1965).

53. V. N. Levkovskii, Soviet Phys. JETP (English Transl.) 18(1), 213-217 (1964).

54. V. Levkovskii, G. E. Kovel'skaya, G. P. Vinitskaya, V. M. Stepanov, and V. V. Sokoz'skii, Soviet J. Nucl. Phys. (English Transl.) 8(1), 4-5 (1969).

55. A. Pasquarelli, Nucl. Phys. A93, 218-222 (1967).

56. E. B. Paul and R. L. Clarke, Can. J. Phys. 31, 267-277 (1952).

57. J. Spaepen, private communication from Albert Fabrey, National Bureau of Standards (1972).